JCI The Journal of Clinical Investigation

Increased apolipoprotein C3 drives cardiovascular risk in type 1 diabetes

Jenny E. Kanter, … , Jay W. Heinecke, Karin E. Bornfeldt

J Clin Invest. 2019. https://doi.org/10.1172/JCI127308.

Research In-Press Preview Metabolism

Graphical abstract

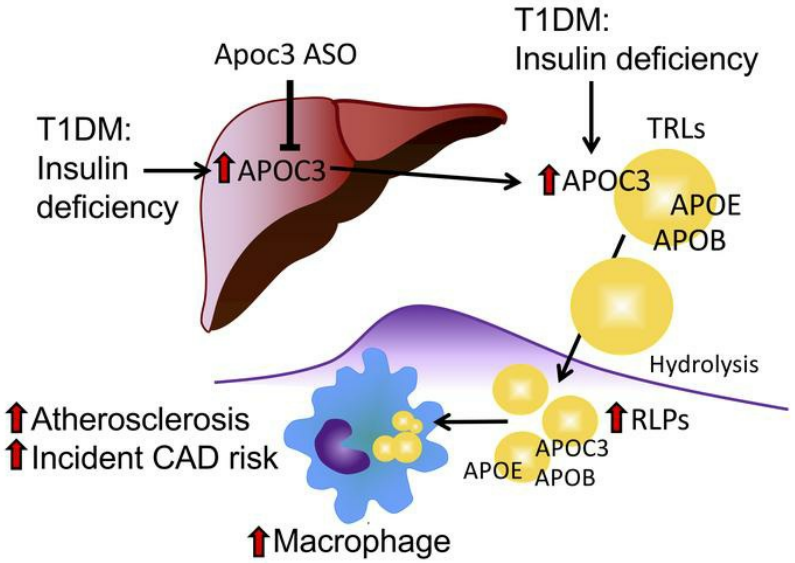

Increased apolipoprotein C3 drives cardiovascular risk in type 1 diabetes

Jenny E. Kanter[1], Baohai Shao[1], Farah Kramer[1], Shelley Barnhart[1], Masami Shimizu-Albergine[1], Tomas Vaisar[1], Mark J. Graham[4], Rosanne M. Crooke[4], Clarence R. Manuel[5], Rebecca A. Haeusler[5], Daniel Mar[3], Karol Bomsztyk[3], John E. Hokanson[6], Gregory L. Kinney[6], Janet K. Snell-Bergeon[7], Jay W. Heinecke[1], Karin E. Bornfeldt[1,2]

Departments of Medicine[1] and Pathology[2], University of Washington Medicine Diabetes Institute, Department of Medicine, Division of Allergy and Infectious Disease[3], University of Washington, Seattle, WA, Ionis Pharmaceuticals[4], Carlsbad, CA, Department of Pathology and Cell Biology[5], Columbia University, Department of Epidemiology, Colorado School of Public Health[6] and Barbara Davis Center for Diabetes[7], School of Medicine, University of Colorado Denver, Aurora, CO

Address correspondence to:

Karin Bornfeldt, University of Washington School of Medicine, Department of Medicine, Division of Metabolism, Endocrinology and Nutrition, 750 Republican Street, Seattle, WA 98109; Email. bornf@uw.edu; Tel. (206) 543-1681

or

Jay Heinecke, University of Washington School of Medicine, Department of Medicine, Division of Metabolism, Endocrinology and Nutrition, 850 Republican Street, Seattle, WA 98109; Email. heinecke@uw.edu; Tel. (206) 221-5366

M.J.G. and R.M.C. are employed by Ionis Pharmaceuticals and provided antisense oligonucleotides for the study. K.E.B. and J.E.K. have received research support from Novo Nordisk A/S for unrelated projects. K.B. is co-founder and equity holder in Matchstick Technologies, Inc, which has licensed the PIXUL technology from the University of Washington. The other authors have declared that no conflict of interest exists.

Figures: 8

Tables: 1

Supplemental figures: 8

Abstract

Type 1 diabetes mellitus (T1DM) increases the risk of atherosclerotic cardiovascular disease (CVD) in humans by poorly understood mechanisms. Using mouse models of T1DM-accelerated atherosclerosis, we found that relative insulin deficiency rather than hyperglycemia elevated levels of apolipoprotein C3 (APOC3), an apolipoprotein that prevents clearance of triglyceride-rich lipoproteins (TRLs) and their remnants. We then showed that serum APOC3 levels predict incident CVD events in subjects with T1DM in the Coronary Artery Calcification in Type 1 Diabetes (CACTI) study. To explore underlying mechanisms, we investigated the impact of Apoc3 antisense oligonucleotides (ASOs) on lipoprotein metabolism and atherosclerosis in a mouse model of T1DM. Apoc3 ASO treatment abolished the increased hepatic *Apoc3* expression in diabetic mice – resulting in lower levels of TRLs – without improving glycemic control. APOC3 suppression also prevented arterial accumulation of APOC3-containing lipoprotein particles, macrophage foam cell formation, and the accelerated atherosclerosis in diabetic mice. Our observations demonstrate that relative insulin deficiency increases APOC3 and that this results in elevated levels of TRLs and accelerated atherosclerosis in a mouse model of T1DM. Because serum levels of APOC3 predicted incident CVD events in the CACTI study, inhibiting APOC3 might reduce CVD risk in T1DM patients.

Introduction

Atherosclerotic cardiovascular disease (CVD) is a major cause of morbidity and mortality in subjects with type 1 diabetes mellitus (T1DM) (1). Although some results suggest that CVD risk associated with diabetes is declining in parallel with the reduced rate of CVD in the general population (2), overall CVD risk remains increased in T1DM patients, especially in premenopausal women, in subjects with sub-optimally controlled blood glucose, and in subjects with features of insulin resistance and metabolic syndrome (3).

The Diabetes Control and Complications Trial (DCCT), a prospective study with a mean follow-up of 6.5 years of microvascular and macrovascular disease in T1DM patients, and its observational follow-up study, the Epidemiology of Diabetes Interventions and Complications (EDIC) study arm, demonstrated that improved glycemic control by intensive insulin therapy associates with long-term reductions in mortality and cardiovascular events (4-6). Moreover, improved plasma lipids and lipoproteins appeared to mediate a significant proportion of the protective effect of more stringent glucose control through intense insulin therapy over time (7).

Lowering low-density lipoprotein-cholesterol (LDL-C) with statins is the best documented strategy for decreasing CVD risk in T1DM, but substantial residual risk remains. The increased risk is often attributed to hyperglycemia, fluctuating glucose levels, or glucose-mediated metabolic memory (8, 9). However, several lines of evidence suggest that glucose does not directly account for the increased CVD risk in diabetes, or at least is not the only risk factor (7, 10, 11). It is likely that

relative insulin deficiency or insulin resistance could explain at least some of the residual CVD risk associated with T1DM.

Accordingly, insulin has been shown to suppress gene expression of apolipoprotein C3 (APOC3) (12, 13), an abundant apolipoprotein that increases triglyceride-rich lipoproteins (TRLs) and their remnants in circulation by blocking their catabolism and clearance (14). Human studies convincingly demonstrate that *APOC3* loss-of-function mutations lower TRL levels and offer cardioprotection (15-20). APOC3 was long believed to elevate plasma TRL levels by inhibiting lipoprotein lipase (14, 21), but a human antisense oligonucleotide (ASO) therapeutic to APOC3 markedly reduced triglyceride levels in lipoprotein lipase-deficient humans with severe hypertriglyceridemia (22). Recent studies in mice and humans indicate that APOC3 regulates multiple steps in TRL metabolism, including inhibiting hepatic uptake of TRLs, slowing the conversion of TRLs to LDL, and inhibiting tissue lipoprotein lipase activity (23-25).

Little is known about the role APOC3 in cardiovascular disease in T1DM patients, in part because T1DM is not usually associated with dyslipidemia (26) while still being associated with increased CVD risk. We therefore tested the hypothesis that APOC3 is a coronary artery disease (CAD) risk factor in T1DM subjects enrolled in the Coronary Artery Calcification in Type 1 Diabetes (CACTI) study, a prospective evaluation of T1DM subjects. Our observations indicated that serum levels of APOC3 predict incident CAD in that cohort, which had normal plasma triglycerides (TGs). We further demonstrated that APOC3 levels are elevated in mouse models of T1DM and that intensive insulin therapy lowers them.

Moreover, we found that lowering APOC3 levels prevents atherosclerosis in a mouse model of T1DM-accelerated atherosclerosis, raising the possibility that APOC3 could be a therapeutic target in T1DM patients.

Results

Serum APOC3 predicts future cardiovascular events in T1DM subjects with normal triglyceride levels. We tested the hypothesis that APOC3 levels predict incident CAD in a case-cohort study of 181 T1DM subjects enrolled in CACTI, a prospective study including a number of measures, including CAD outcomes (myocardial infarction, coronary artery bypass grafting, angioplasty, or CAD death based on medical records). All subjects were apparently healthy and without known CAD when samples were collected. Serum APOC3 levels were quantified by targeted mass spectrometric analysis. The clinical characteristics of the case and cohort groups are shown in Table 1. Although the cohort's plasma levels of TGs were normal, scatterplot analyses showed a positive correlation between serum APOC3 levels and TG levels (r^2=0.33; p<0.0001). There were no significant correlations between APOC3 and LDL-C or HDL-C (p=0.23 and p=0.27, respectively).

TG levels predicted incident CAD risk with a hazard ratio of 1.50 (95% confidence interval [CI] 1.18-1.90; p=0.001; Figure 1). However, serum APOC3 was a stronger predictor, with a hazard ratio of 1.84 (95% CI 1.40-2.40; p<0.0001). In three different models — model 1, a logistic regression model (Figure 1) adjusted for age, sex, and diabetes duration; model 2, in which model 1 was further

adjusted for non-lipid factors (HbA1c, blood pressure, and current smoking status); and model 3 in which model 1 was further adjusted for lipid factors (LDL-C and HDL-C) — each SD increase in serum APOC3 remained associated with a highly significant 1.8- to 2.0-fold risk for CAD (Figure 1). Thus, serum APOC3 predicted CAD events in subjects with T1DM and TGs in the normal range independently of LDL-C and HDL-C. When model 1 was adjusted for log TG levels (model 4; Figure 1), the hazard ratio was 1.45 (p=0.11). Therefore, the effects of APOC3 and TGs on CAD in adults with T1DM are not independent.

To further interrogate the relationship between APOC3 and TGs, we determined whether adding TGs to a model already adjusted for APOC3, age, sex and diabetes duration improved the fit of the model, based on the change in the -2 log likelihood (-2LL). The addition of TGs did not significantly improve the model fit that included APOC3 (change in -2LL = 2.368, p=0.12). In contrast, adding APOC3 to a model that included TGs, age, sex, and diabetes duration significantly improved model fit (change in -2LL = 3.941, p=0.047). This approach indicates that APOC3 is a stronger predictor of CAD than TGs in a model adjusted for age, sex, and diabetes duration.

Relative insulin deficiency increases APOC3 levels in mouse models of T1DM. To determine mechanisms whereby APOC3 might be increased in T1DM, we used two independent mouse models of T1DM: (i) destruction of β-cells mediated by CD8+ T cells induced by a virus (27, 28) and (ii) β-cell injury induced by streptozotocin (STZ) (29). All the mice were deficient in the LDL receptor (*Ldlr*

$^{-/-}$) to mimic a more human-like lipoprotein profile and were fed a low-fat semi-purified diet to avoid marked hypercholesterolemia (27).

Plasma APOC3 levels correlated with plasma TG levels in both diabetic mice (r^2=0.37, p<0.0001, n=53) and non-diabetic mice (r^2=0.07, p=0.04, n=59). In the virally-induced T1DM model, diabetes resulted in a higher ratio of plasma APOC3 to TG levels. The APOC3:TG ratio was 3.4 ± 0.3 (mean ± SEM, n=42) in non-diabetic mice versus 4.8 ± 0.5 in diabetic mice (p=0.009; n=36). Accordingly, at any given TG level within the range of 96-460 mg/dL, plasma APOC3 levels were 1.75- to 1.95-fold higher in diabetic mice, as compared with non-diabetic littermates, independent of blood glucose (Figure 2A). Although we did not directly measure APOC3 production or clearance rates, these observations strongly suggest that levels of APOC3 are higher in the mouse model of T1DM than in non-diabetic mice, and that the increased APOC3 levels did not simply reflect increased TG levels.

Studies on isolated hepatocytes suggest that hyperglycemia can increase APOC3 production (30). We therefore determined if dapagliflozin, an inhibitor of sodium glucose transporter 2 (SGLT2), affected APOC3 and lipid levels in mice with STZ-induced diabetes. This model was used because STZ-diabetic mice retain some endogenous insulin production. Dapagliflozin reduces blood glucose through insulin-independent renal excretion of glucose. It lowered blood glucose without significantly affecting plasma TGs, cholesterol, or plasma APOC3 (Figure 2B-E).

The *APOC3* promoter contains an insulin response element (13), and high doses of insulin have been shown to suppress hepatic *Apoc3* gene expression in STZ-diabetic mice (12). To test if the elevation in plasma APOC3 we observed in diabetic mice was driven by insulin deficiency, we quantified levels of APOC3, lipids, and glucose in mice with virus-induced diabetes that were either conventionally treated with insulin (sufficient to prevent extensive weight loss and ketonuria) or with an intense insulin regimen to normalize blood glucose. Blood glucose levels were significantly lower in the diabetic mice on intense insulin therapy than in the conventionally treated diabetic mice (Figure 2F and Figure S2E). The mice on intense insulin therapy also had significantly lower plasma APOC3 levels. In contrast, intense insulin therapy did not alter plasma cholesterol or TG levels (Figure 2G-I). Nuclear exclusion of the transcription factor FoxO1 has been proposed to mediate the suppressive effects of insulin on *Apoc3* expression (31). To determine if *Apoc3* is regulated by FoxO transcription factors we measured *Apoc3* mRNA in mice with liver-targeted deletions of FoxO1, FoxO3 and FoxO4 (Figure S1A), using a previously described model (32). Contrary to experiments based on forced overexpression of FoxO1 (31), hepatocyte deletion of FoxOs did not alter *Apoc3* mRNA levels in mice fasted for 4 h during the dark cycle (Figure S1B). Consistent with this, injecting adult FoxO triple floxed mice with an adeno-associated virus (AAV-*Tbg*-Cre) to induce hepatic FoxO deletion successfully decreased *Foxo1* mRNA in the liver by 86% (P=0.009), but did not affect *Apoc3* mRNA (1.00 ± 0.14 vs 1.05 ± 0.08, p=0.77).

To further address whether insulin acts by suppressing transcription of hepatic *Apoc3*, we took advantage of a new microplate-based chromatin immunoprecipitation (ChIP) platform to analyze livers from non-diabetic mice, diabetic mice and diabetic mice treated with the intense insulin regimen or an acute injection of insulin. We analyzed polymerase II (pol II) binding to the *Apoc3* promoter and enhancer and histone H3 modifications associated with active and inactive chromatin. Insulin injections reduced blood glucose levels and induced phosphorylation of Akt and GSK3β in livers of diabetic mice, as would be expected (Figures S2A-B). Furthermore, insulin resulted in increased pol II binding to the glucokinase (*Gck*) promoter, a known hepatic target of physiological insulin levels in vivo (33) (Figures S2C-D). However, insulin did not alter binding of pol II or modified histones to the *Apoc3* promoter or enhancer (Figures S2C-D) after an acute insulin injection (30 min) or in the intense insulin treatment experiment in which a marked reduction of plasma APOC3 was observed (Figure 2I). The suppressive effect of insulin on plasma APOC3 levels had a much slower onset than the rapid blood glucose-lowering effect of insulin (Figures S2E-F), consistent with the reported half-life of plasma APOC3 (34).

Collectively, these experiments support the conclusion that transcriptional regulation of *Apoc3* constitutes a minor pathway for its regulation by diabetes and insulin and that plasma APOC3 levels are elevated in T1DM primarily due to insulin deficiency rather than because blood glucose levels are elevated.

Apoc3 antisense oligonucleotide treatment reduces APOC3 and TRL levels in diabetic mice. To explore the contribution of elevated levels of APOC3 to accelerated atherosclerosis in our virus-induced mouse model of T1DM (27), we used a mouse specific Apoc3 ASO that has been shown to significantly reduce APOC3 and TG levels in multiple rodent models (23, 35). Our four groups of mice were (i) non-diabetic control mice treated with a control ASO, (ii) non-diabetic control mice treated with the Apoc3 ASO, (iii) diabetic littermates treated with the control ASO, and iv) diabetic littermates treated with the Apoc3 ASO. The mice received the ASO i.p. twice weekly for 12 weeks, starting 2 days after the onset of diabetes (glucose > 250 mg/dL).

Plasma glucose levels were similarly elevated in the diabetic mice treated with a control ASO or Apoc3 ASO (Figure 3A). Apoc3 ASO treatment lowered plasma cholesterol levels in both the non-diabetic and diabetic mice (Figure 3B), and it also lowered plasma TG levels in the diabetic mice (Figure 3C). At the end of the study, we measured hepatic and intestinal *Apoc3* mRNA levels in the four mouse groups. The diabetic mice had modestly higher levels of hepatic *Apoc3* mRNA than the non-diabetic controls (Figure 3D), consistent with increased APOC3 production, although plasma levels of APOC3 were increased to a much greater extent by diabetes. The Apoc3 ASO markedly suppressed hepatic *Apoc3* mRNA levels in both non-diabetic and diabetic mice (Figure 3D). There were no significant effects of diabetes or the Apoc3 ASO on intestinal levels of *Apoc3* mRNA (Figure S3A), as in previous studies that found a less pronounced effect of Apoc3 ASO in the intestine than in the liver (35). These findings are most likely

explained by lower distribution of ASO to the intestine. The Apoc3 ASO did not alter hepatic TG levels or plasma ALT (alanine aminotransferase) levels (Figure S3B-C), indicating that this ASO is well tolerated; results that are consistent with previous human and animal studies (35).

Plasma lipoprotein profiles demonstrated that Apoc3 ASO primarily suppressed the increased levels of VLDL cholesterol and VLDL triglycerides (TRLs), with a smaller effect on IDL/LDL cholesterol (Figure 3E-F). Analysis of plasma APOC3 levels by ELISA and targeted mass spectrometry confirmed that diabetes associated with a significant increase in plasma APOC3 levels and that the Apoc3 ASO markedly suppressed plasma APOC3 levels in both non-diabetic and diabetic mice (Figure 3G-H, S4A).

To get a fuller picture of how diabetes and Apoc3 ASO alter lipid metabolism, we measured several other plasma apolipoproteins by targeted mass spectrometry. Diabetes increased plasma APOE levels more than 2-fold over those in non-diabetic mice (Figure 4A and Figure S4B), an effect that Apoc3 ASO completely prevented. Previous studies have shown that Apoc3 ASO treatment lowers APOE-rich TRLs in non-diabetic human subjects (20), suggesting that diabetes increases levels of APOE-containing TRLs and their remnants that are normalized by the Apoc3 ASO. Interestingly, the effect of diabetes on APOB plasma levels was much less pronounced: the difference reached statistical significance only when a peptide present in both APOB100 and APOB48 was quantified (Figure 4B-C). This suggests that diabetes did not significantly increase the number of APOB100-containing lipoprotein particles and that the Apoc3 ASO

did not lower these particles, also consistent with data in non-diabetic human subjects (20). The effects of diabetes on plasma APOA1 (HDL's major protein) were modest (Figure 4D). We also observed no effect of diabetes or Apoc3 ASO on HDL levels and function that could explain the atheroprotective effects of Apoc3 ASO (see below), despite an almost complete loss of APOC3 associated with HDL in Apoc3 ASO-treated mice (Figure S5). Consistent with an insignificant role for HDL relative to TRLs in mediating the effect of APOC3, HDL-associated APOC3 was a much weaker CAD risk predictor than was serum APOC3 in the human CACTI cohort, with a non-significant hazard ratio of 1.38 (95% CI 0.93-2.05, p=0.11) in the model adjusted for age, diabetes duration and sex.

Furthermore, in diabetic mice we observed a modest increase in APOA4 and a marked increase in plasma APOC2, a potent activator of lipoprotein lipase. Antisense inhibition of APOC3 suppressed the increase in APOC2 in the diabetic mice (Figure 4E-F), also consistent with human data on subjects without diabetes (20).

Together, these results support the proposal that diabetes primarily affects TRL metabolism, rather than other lipoproteins, and that Apoc3 ASO's impact on TG levels is mediated in large part by reduced levels of APOE-containing TRLs and their remnants in diabetic mice, which is consistent with other mouse and human studies (20, 24, 36). In contrast, HDL containing APOA1 and LDL containing APOB100 were not markedly affected by diabetes or Apoc3 ASO in our mouse model. The inability of Apoc3 ASO to increase HDL might be due to the

lack of cholesteryl ester transfer protein in rodents (37), as antisense inhibition of APOC3 increases HDL levels concomitant with TG lowering in humans (38, 39).

Apoc3 ASO prevents diabetes-accelerated lesion initiation and macrophage accumulation in artery walls. In order to investigate whether the effects of Apoc3 ASO on lipids translate to reduced atherosclerosis, we quantified atherosclerosis at two vascular sites in all four groups of mice (non-diabetic and diabetic mice injected with the control ASO and non-diabetic and diabetic littermates injected with the Apoc3 ASO). Lesions in the aorta, from the arch to the iliac artery bifurcation, were analyzed *en face* and identified as areas positive for the lipophilic stain Sudan IV (Figure 5A). Diabetic mice had larger lesions in the aorta, as demonstrated previously (27, 40). Administration of the Apoc3 ASO completely prevented the increase in lesion area in the diabetic mice (Figure 5B). Lesions in the brachiocephalic artery (BCA) were analyzed by serial sectioning of the entire BCA and measuring cross-sectional lesion area at the site of maximal extent (27, 41). Like in the aorta, diabetes promoted atherosclerosis in the BCA, and this effect was prevented by the Apoc3 ASO (Figure 5C-E). The BCA lesions were early fatty streak lesions consisting primarily of macrophages. Diabetes increased macrophage lesion area (measured by Mac-2 immunohistochemistry), and Apoc3 ASO prevented the increase (Figure 5F).

Monocytosis can promote atherosclerosis in non-diabetic and diabetic hypercholesterolemic mice (42-44). We therefore quantified levels of circulating leukocyte populations by flow cytometry to determine if the Apoc3 ASO

suppressed blood monocyte levels. Neither diabetes nor the Apoc3 ASO altered levels of white blood cells, monocytes, Ly6C^{hi} monocytes, or neutrophils (Figure S6A-D). Diabetic mice had elevated platelet levels, as in recent studies (45), but administration of the Apoc3 ASO had no significant effect on platelets in our animals (Figure S6E). Altered levels of circulating monocytes are therefore unlikely to explain the effect of Apoc3 ASO on lesional macrophage accumulation and atherosclerosis in this mouse model of diabetes.

SAA1 and SAA2 are prominent acute phase proteins in mice, which have very low levels of CRP, the major human acute phase protein (46). Apoc3 ASO modestly increased SAA levels in our diabetic mice (Figure S6F). We also found that peritoneal macrophages from the diabetic mice exhibited increased inflammatory activation, consistent with our previous studies (40). However, Apoc3 ASO did not significantly lower *Tnfa* and *Il1b* mRNA levels in peritoneal macrophages of the diabetic mice (Figure S6G-H).

Together, these results suggest that the pro-atherosclerotic effects of APOC3 in diabetic mice reflect increased macrophage accumulation in the artery wall rather than altered levels of circulating myeloid cells or systemic inflammation.

Apoc3 ASO treatment prevents the accumulation of APOC3, APOE and APOB in artery walls and macrophage foam cell formation in diabetic mice. Deposition of pro-atherogenic lipoproteins in the artery wall is a key step in atherogenesis (47). We therefore asked if arterial accumulation of APOC3-containing lipoproteins is enhanced in diabetic mice. Immunostaining of

atherosclerotic lesions, using an antibody to APOC3 (Figure S7), revealed larger amounts of APOC3 in the BCA of diabetic mice and complete reversal of this pathology by Apoc3 ASO (Figure 5C, G). Interestingly, APOC3 was detected both in the arterial media, just below the internal elastic lamina and sites of accumulated macrophages, and around macrophages in the intima (Figure 5C). Furthermore, immunohistological staining of adjacent cross-sections revealed similar patterns for APOE and APOB (Figure 5C, G-I). Importantly, diabetes resulted in increased APOB in the artery wall without significantly affecting plasma APOB100 levels (Figure 4B). These observations suggest that APOC3 promotes the trapping of atherogenic lipoproteins—likely remnant particles containing APOC3, APOE and APOB—in the artery wall.

To further investigate the role of foam cell formation in diabetic mice, we harvested peritoneal macrophages and quantified levels of cholesterol and cholesteryl ester. Macrophages from the diabetic mice had elevated levels of cholesteryl ester—but not total cholesterol—and cholesteryl ester levels were normalized in macrophages harvested from the diabetic mice we treated with the Apoc3 ASO (Figure 6A-B). The accumulation of cholesteryl ester in macrophages from the diabetic mice likely resulted from increased levels of lipoproteins/remnants containing cholesterol and APOC3 in the animals' peritoneal interstitial fluid. These levels decreased markedly after Apoc3 ASO treatment (Figure 6C-D).

Together, these results suggest that the beneficial effects of Apoc3 ASO on atherosclerosis in the setting of diabetes are due to reduced levels of APOC3,

APOE and APOB-containing lipoproteins/remnants within the artery wall, and a subsequent reduction in macrophage foam cells.

Apoc3 ASO treatment reduces necrotic core size in diabetic mice with pre-existing lesions. To investigate if APOC3 accumulation is also increased in more complex lesions under diabetic conditions we initiated lesion formation by fat-feeding for 12 weeks prior to inducing diabetes (Figure S8A). Diabetes was subsequently induced, and the mice were maintained for an additional 4 weeks (Figure S8A). Diabetes resulted in hyperglycemia and a modest increase in plasma cholesterol (Figures S8B-C). Consistent with our other results, plasma TG levels were 108 $\pm$ 11 mg/dL in non-diabetic mice and 402 $\pm$ 87 mg/dL in diabetic mice (mean $\pm$ SEM; n=9-10; p=0.0056) and plasma APOC3 levels were 454 $\pm$ 37 μg/mL in non-diabetic mice and 1531 $\pm$ 162 μg/mL in diabetic mice (mean $\pm$ SEM; n=9-10; p<0.00001). The short duration of diabetes did not alter atherosclerotic lesion size of pre-existing lesions in the aortic sinus (Figures S8D-E). We have previously demonstrated that diabetes results in a more severe lesion phenotype of pre-existing lesions (28), and consistently, after only 4 weeks of diabetes the mice exhibited an increased necrotic core size (Figures S8D and S8G). This lesion phenotype was associated with a dramatic increase in lesional APOC3 accumulation (Figures S8D and S8H).

Next, to test if Apoc3 ASO treatment could prevent progression of advanced lesions characterized by the increased necrotic cores in diabetic mice, pre-established lesions were induced by fat-feeding for 12 weeks followed by induction

of diabetes and treatment with Apoc3 ASO or control ASO. As shown in Figures 7A-D, Apoc3 ASO treatment did not alter blood glucose levels, but modestly suppressed plasma cholesterol, and markedly suppressed TGs and plasma APOC3 levels, similar to the results of the lesion initiation study (Figure 3). Apoc3 ASO treatment did not reduce total lesion size or macrophage accumulation as assessed by Mac-2 staining in pre-existing lesions (Figures 7E-G). Strikingly, Apoc3 ASO treatment significantly reduced lesional APOC3 accumulation and necrotic core size (Figures 7E and 7I-K), suggesting that inhibition of APOC3 prevents the progression of lesions into more advanced lesions characterized by larger necrotic cores.

Discussion

Our observations indicate that serum levels of APOC3 predict incident CAD risk in T1DM subjects with normal TG levels (<150 mg/dL) independently of LDL-C, HDL-C and multiple other non-lipid risk factors, including diabetes duration and HbA1c. When we adjusted the model for TGs, APOC3 was no longer a significant predictor of CAD, likely reflecting the strong links between APOC3 and TGs. However, adding APOC3 to an analysis that adjusted for TGs, age, sex, and diabetes duration significantly improved the fit of the model to the data. In contrast, adding TGs to an analysis that adjusted for APOC3 did not improve the model fit. Taken together, these observations support the proposal that elevated levels of APOC3 are a risk factor for CAD in patients with T1DM and normal TG levels and that although APOC3 and TGs are not independent, APOC3 is a stronger predictor of CAD than are TGs in this cohort of subjects with T1DM.

Importantly, our mouse studies demonstrated that diabetes increases plasma levels of APOC3. Moreover, lowering APOC3 levels with an ASO to APOC3 markedly reduced atherosclerosis in diabetic mice, likely by reducing levels of atherogenic lipoproteins containing APOC3, APOE and APOB. These findings raise the possibility that APOC3 could be a therapeutic target in humans with T1DM.

What could explain a heightened importance of APOC3 as a CAD risk factor in T1DM? Previous mouse studies have failed to demonstrate a beneficial effect of APOC3-deficiency on atherosclerosis in non-diabetic mice fed an atherogenic diet (48). Our findings that plasma APOC3 levels were ~2-fold higher in diabetic

mice than in control mice over a wide range of TG levels, and that hepatic *Apoc3* expression was likewise increased in diabetic mice shed light on this question. These results suggest that plasma APOC3 levels are elevated not simply due to increased retention of TRLs in plasma, but through a mechanism tied to the T1DM condition. Hepatic *Apoc3* transcription has been shown to be increased by elevated glucose through the transcription factors HNF-4α and ChREBP in cultured cells (12, 30). However, hyperglycemia was not responsible for the elevated plasma APOC3 levels in our diabetic mouse models as we used an SGLT2 inhibitor to normalize blood glucose levels and found no significant reduction in APOC3 levels. Instead, we found that intensive insulin therapy significantly reduced plasma levels of APOC3.

Forced overexpression of FoxO1 has been demonstrated to induce hepatic *Apoc3* expression (31) and FoxO1 is believed to mediate the effects of insulin on *Apoc3* expression. However, our data using mice deficient in all FoxOs in the liver suggest that neither FoxO1, FoxO3 or FoxO4 are required for hepatic *Apoc3* expression. Furthermore, PIXUL-ChIP (49) analyses of *Apoc3* transcriptional regulation in diabetic and insulin treated diabetic mice failed to reveal significant transcriptional regulation of *Apoc3*. Together, these results demonstrate that the marked increase in plasma APOC3 in diabetic mice and the normalization by intense insulin treatment are likely mediated by post-transcriptional effects or by altered kinetics of plasma APOC3. One possibility is that insulin reduces plasma APOC3 levels by increasing hepatic uptake of remnant lipoproteins through translocation of LDLR-related protein 1 (50), a protein involved in APOC3

clearance (23). The exact mechanism of insulin suppression of APOC3 in the setting of diabetes is an interesting area of future studies. We have previously shown that intensive insulin therapy prevents atherosclerosis in our virally-induced mouse model of T1DM-accelerated atherosclerosis (27), consistent with a role for relative insulin deficiency in promoting atherosclerosis in T1DM.

Volanesorsen, a human APOC3 antisense drug, effectively lowers plasma TG levels in humans with markedly elevated TG levels due to lipoprotein lipase-deficiency without lowering LDL cholesterol (22). This antisense therapeutic agent also reduces TG levels in subjects with type 2 diabetes mellitus and in subjects with hypertriglyceridemia and dyslipidemia (38, 39). A pilot study suggested that volanesorsen is also effective in subjects with normal TG levels (35). Our findings suggest that elevated levels of APOC3 at least partly explains the increased risk of CAD in T1DM in patients with normal TGs, and that an APOC3 ASO might significantly reduce APOC3 levels—and perhaps CVD risk—in those subjects. In future studies, it will be important to investigate the relationship between glycemic control, insulin sensitivity and APOC3 levels in both T1DM and T2DM subjects.

What is the mechanism whereby increased APOC3 accelerates atherosclerosis in diabetes? We found elevated levels of APOE in proteolytic digests of plasma proteins of our diabetic mice, strongly suggesting that elevated levels of APOC3 increase levels of atherogenic TRL remnant lipoproteins rich in APOE and APOB. Consistent with this proposal, we found that the elevated APOE levels in diabetic mice were normalized by treatment with the Apoc3 ASO. Previous mechanistic studies demonstrated that APOC3 blocks clearance by the

liver of lipoproteins containing APOE, perhaps by interfering with APOE-mediated hepatic uptake of those lipoproteins (51-53). In contrast, we found no evidence that APOC3 promotes systemic inflammation. Nor did we find any evidence of increased circulating levels of monocytes in diabetic mice.

Instead, elevated APOC3 likely acts in diabetes by promoting the accumulation of atherogenic lipoproteins containing APOC3, APOE, and APOB in the artery wall. An attractive hypothesis is that lipoprotein remnants containing APOC3, APOE and APOB are trapped in the artery wall, which would in turn increase monocyte recruitment and the accumulation of macrophage foam cells in lesions. Our demonstration that APOC3 accumulates in macrophage-rich regions of both early and advanced atherosclerotic lesions and in medial areas below lesions is consistent with this proposal (Figure 8). It is possible that APOC3 enhances the binding of APOB-containing lipoproteins to extracellular matrix (54, 55), or that the increased presence of atherogenic lipoprotein remnants in the artery wall is responsible for accelerated atherosclerosis. More research is needed to address whether the atherogenic effects are due to direct effects of APOC3 or to atherogenic effects of a particular APOC3-containing lipoprotein particle. We also found that APOC3 levels increased in the interstitial peritoneal fluid of diabetic mice and that peritoneal macrophages of diabetic mice had increased levels of cholesteryl ester, the biochemical hallmark of macrophage foam cells. Our observations are consistent with the “response-to-retention” hypothesis of Williams and Tabas (47), which suggests that retention of cholesterol-rich lipoproteins in the artery wall provokes a cascade of responses that initiate and advance

atherosclerosis. Our data further suggest that increased arterial retention of APOC3, APOE and APOB-containing lipoproteins is responsible for the increased atherosclerosis initiation and progression in the setting of diabetes.

Collectively, our observations raise the possibility that APOC3 is an important risk factor for atherosclerotic CVD in T1DM patients with normal TG levels and that lowering of APOC3 levels might reduce the excess risk for CVD observed in those subjects.

Methods

CACTI study participants and clinical measurements. The Coronary Artery Calcification in Type 1 Diabetes (CACTI) study has been described previously (56). Briefly, 1,416 participants, 19–56 years of age, have been followed prospectively at the University of Colorado for a variety of endpoints, including calcium artery score and CVD events. None of the subjects had a known history of CVD, including angina, coronary artery bypass graft, and coronary angioplasty, but they all had been diagnosed with T1DM before age 30, or had positive autoantibodies or a clinical course consistent with T1DM, and had been treated with insulin within 1 year of diagnosis. The mean duration of diabetes was 23 years at enrollment, and the minimum was 4 years. After an overnight fast, blood was collected and centrifuged, and separated plasma and serum were stored at 4°C until assay. Total cholesterol and TG levels were measured using standard enzymatic methods. HDL-C was separated using dextran sulfate, and LDL-C was calculated using the Friedewald formula. High-performance liquid chromatography was used to measure HbA1c (HPLC; BioRad variant).

We designed a case-cohort study to test the pre-specified hypothesis that elevated serum APOC3 predicts CAD events in subjects with T1DM. CAD events were defined as myocardial infarction, coronary artery bypass grafting, angioplasty, or CAD death based on medical records. Events were ascertained through annual surveillance questionnaires sent to all study participants, through medical history questionnaires assessed at all in-person visits, through reports of events made by study participants, family members and physicians, and through

mortality surveillance. Death searches were performed through the Colorado Department of Public Health Vital Records department and through the National Death Index (NDI) database. Medical records were requested for all events that occurred in a medical facility. Adjudication of events was performed by blinded analysis of those records by a Morbidity and Mortality Committee comprised of three physicians. The subcohort consisted of 145 subjects with T1DM randomly selected from the overall CACTI cohort, which included 11 of the CAD cases. Cases were 47 subjects with CAD events which occurred after baseline blood collection. All subjects enrolled in CACTI who had had an adjudicated CAD event were included in the analysis. All the subjects were free of known CAD at the time of blood collection. One subject of the 181 was on TG-lowering medication (gemfibrozil). The clinical characteristics of the two groups are listed in Table 1. The risk for a CAD event was modeled using weighted Cox proportional hazards linear regression. Strata were analyzed for each CAD event, with subcohort subjects serving as controls for each CAD event strata that occurred while the subcohort member remained at risk for a CAD event (e.g. prior to experiencing a CAD event and prior to censoring). The log-likelihood ratio test was used to determine change in model fit when adding TGs and APOC3 to the adjusted models. The strength of the association was evaluated using hazard ratio.

Mouse models of T1DM-accelerated atherosclerosis. The T cell-induced LDL receptor-deficient (*Ldlr*$^{-/-}$) *Gp*^{Tg} mouse model of T1DM-accelerated atherosclerosis has been described previously (27). These mice express the lymphocytic

choriomeningitis virus (LCMV) glycoprotein (GP) under control of the insulin promoter, allowing reliable induction of diabetes due to $CD8^+$ T cell-mediated β-cell destruction following LCMV injection. In the current study, female *Ldlr*$^{-/-}$;*Gp*^{Tg} mice on the C57BL/6J background, 10–14 weeks of age, were injected with LCMV. Non-diabetic littermates were injected with saline. At the onset of diabetes (defined as blood glucose levels >250 mg/dL) 10 days after LCMV injection, the non-diabetic and diabetic mice were fed a low-fat semi-purified diet without added cholesterol, as previously described (27). The diabetic mice received subcutaneous insulin pellets to provide baseline insulin, and were treated with insulin glargine (Linshin Canada Inc., Toronto, ON and Lantus®, Sanofi, Bridgewater, NJ, respectively) to prevent weight loss and ketonuria as needed. The second mouse model of diabetes-accelerated atherosclerosis used in this study was the streptozotocin (STZ) *Ldlr*$^{-/-}$ model, also described previously (29). Diabetes was induced in male *Ldlr*$^{-/-}$ mice by intraperitoneal injection of STZ (mixed anomers no. S0130, 50 mg/kg; Sigma-Aldrich) dissolved in freshly made 0.1 M sodium citrate buffer, pH 4.5) for 5 consecutive days. Controls were injected with vehicle citrate buffer. Diabetes was defined in these mice as described above, and the animals were treated with insulin glargine as needed to prevent significant weight loss and ketonuria. A subset of the STZ-diabetic mice was treated with the SGLT2 inhibitor dapagliflozin at 25 mg/kg/day in the drinking water to reduce blood glucose levels, based on the method described by Nagareddy et al. (42). Water intake was measured initially to verify dosing. To test the effect of an intense insulin regimen on plasma APOC3 levels, we injected female *Ldlr*$^{-/-}$; *Gp*^{Tg} mice with LCMV

to induce diabetes. At the onset of diabetes, the mice were allocated into either conventional treatment (see above) or intense insulin treatment. For intense treatment, the mice received insulin via insulin pellets as well as 3 daily injections (7 hours apart) of insulin glargine, with the goal of keeping the mice normoglycemic (<200 mg/dL) for 9 days. The mice were euthanized in the morning 10 hours after their last insulin injection. Another group of mice were rendered diabetic with LCMV, maintained for 10 days, followed by a subset of mice receiving an acute injection of insulin 30 minutes prior to euthanasia (0.2-0.3 U/ mouse). Prior to the acute injection, blood glucose and plasma APOC3 levels were similar between the two diabetic groups and were elevated compared to the non-diabetic mice. For both the SGLT2 inhibitor and intense insulin experiment, mice were randomized to treatment groups by similarity of initial blood glucose level.

To study atherosclerotic lesion initiation, mice were rendered diabetic and maintained for 12 weeks on a low-fat semi-purified diet (27, 40). For studies of pre-existing lesions, mice were first fed a high-fat, semi-purified diet (40% calories from fat, 1.25% cholesterol) (27, 28) for 12 weeks, and were then switched to normal mouse chow (to reduce plasma cholesterol) and then injected with LCMV to induce diabetes. Once diabetes had developed, the mice were fed the low-fat semi-purified diet and maintained for an additional 4 weeks (Figure S8A).

At the end of the subsets of experiments, we isolated macrophages from the peritoneal cavity, using ice-cold PBS + 5 mM EDTA. The macrophages were allowed to adhere for 1 hour before they were harvested for either RNA isolation (Nucleospin RNA plus; Macherey-Nagel, Bethlehem, PA) or measurements of total

cholesterol, free cholesterol, and cholesteryl esters (Amplex Red Cholesterol assay, ThermoFisher, Grand Island, NY).

Apoc3 ASO treatment. The mouse-specific Apoc3 ASO (5' CCAGCTTTATTAGGGACAGC-3') and a control ASO (CCTTCCCTGAAGGTTCCTCC) were 20 nucleotide 5-10-5 2'-O-methoxyethyl (MOE) gapmers, with underlining indicating 2'MOE modified bases, produced by Ionis Pharmaceuticals (35). The ASOs (25 mg/kg) were injected i.p. twice weekly, starting 2 days after the onset of diabetes. ASO doses were adjusted every 2 weeks based on body weight. The ASOs were well tolerated in mice.

Analysis of glucose and lipid metabolism. Blood glucose was measured in the saphenous vein blood by stick tests (One touch Ultra). As the glucometer does not go beyond 600 mg/dl; values above that are set to 600 mg/dl. Plasma cholesterol levels were determined by the Cholesterol E kit (Wako Diagnostics, Wako, TX), and plasma and liver TGs were determined by a colorimetric kit from Sigma-Aldrich. Plasma lipoprotein profiles were analyzed by fast protein liquid chromatography (FPLC), as described previously (27). Cholesterol and TGs were measured in each fraction. HDL functional assays and analysis of HDL particle concentration were performed as described in the Supplement. To test for hepatotoxicity, we measured plasma levels of the liver enzyme alanine aminotransferase (ALT) with a kit from Sigma (MAK052-1KT). Plasma APOC3

levels were measured using an APOC3 ELISA from Abcam (ab217777; Cambridge, MA) and were verified using targeted mass spectrometry (see below).

Quantification of atherosclerosis. The aorta was dissected after *in situ* perfusion with PBS, and was fixed in 10% phosphate-buffered formalin (Sigma-Aldrich). Aortas were opened longitudinally (from the heart to the iliac bifurcation), and an investigator blinded to the treatment groups quantified the extent of atherosclerosis *en face* after Sudan-IV staining, as previously described (27, 40). Brachiocephalic arteries (BCAs) and aortic sinuses were cross-sectioned and stained with the Movat's pentachrome stain to visualize lesion morphology. The aortic sinus was analyzed at 3 separate sites beginning at the appearance of all 3 aortic valve leaflets (57). Lesional macrophages were visualized by Mac-2 immunohistochemistry, using a monoclonal rat anti-mouse Mac-2 antibody (CL8942AP at 1 μg/ml; Cedarlane, Burlington, NC) (28). APOC3 immunohistochemistry was carried out with a rabbit polyclonal APOC3 generated by Ionis Pharmaceuticals (1:1000 dilution). APOB immunohistochemistry was carried out using a biotinylated goat-anti APOB antibody (R&D Systems, BAF3556; at 1:50) and APOE immunohistochemistry was carried out using a rabbit monoclonal antibody (Abcam, ab183597; at 1:2000). Negative isotype controls (or serum controls) of the same concentrations or dilutions were used as controls (Figure S7).

Flow cytometry of blood leukocytes. Mice were bled from the retro-orbital plexus under isoflurane sedation after 12 weeks of diabetes. EDTA was the anti-coagulant. Total leukocytes were measured using an automated cell counter for mouse blood samples (Hemavet; Drew Scientific, Oxford, CT). For flow cytometric analysis, erythrocytes were lysed with an ammonium-chloride-potassium buffer and discarded, and leukocytes were stained using a fixable viability dye, CD45, CD115, and GR1 (clones 30-F11, AFS98 and RB6-8C5, respectively; eBioscience, now ThermoFisher). Monocytes were identified as CD115-positive cells, and neutrophils were identified as CD115-negative $GR1^{hi}$ cells. All analyses were performed with live, single, CD45-positive cells. The monocytes were further divided into GR^{hi} ($Ly6C^{hi}$) and $GR1^{lo}$ ($Ly6C^{lo}$) subpopulations. The cells were analyzed on a BD FACS RUO flow cytometer (BD Bioscience, Franklin Lakes, NJ). Flow cytometric analysis was normalized to total white blood cell counts (WBC) and expressed as cells/mL of blood, using the assumption that all WBC are CD45-positive.

Real-time PCR. Gene expression in liver, intestine, and resident peritoneal macrophages was quantified by real-time PCR. RNA isolation and the real-time PCR protocol were performed as described previously (40). Briefly, RNA was isolated using Qiagen (Valencia, CA) RNeasy or Macherey-Nagel (Bethlehem, PA) Nucleospin RNA kits according to the manufacturers' protocols. RNA samples were treated with DNase1 (1 µg/sample, Thermoscientific, Waltham, MA) to remove traces of DNA. Real-time PCR was performed using the SYBR Green 1

detection method (Thermoscientific). Cycle threshold (Ct) values were normalized to *Rn18s* and presented as fold over control. Primer sequences are available upon request.

Liquid chromatography-electrospray ionization tandem mass spectrometric analysis of serum, plasma and HDL-associated proteins. Liquid chromatography-electrospray ionization targeted tandem mass spectrometric (LC-ESI-MS/MS) analysis was used to determine selected proteins in human serum, mouse plasma and human and mouse HDL, as described below and in the Supplement.

Digestion of human serum. In a digestion plate, 5 µL of serum was diluted in 245 µL of 25 mM NH_4HCO_3. An aliquot of 10 µL of the diluted serum (equivalent to 0.2 µL of serum and ~14 µg protein) was placed into a new digestion plate. Following the addition of freshly prepared methionine (5 mM final concentration), in 20% acetonitrile and 100 mM NH_4HCO_3, serum proteins (~14 µg) were reduced with dithiothreitol and then alkylated with iodoacetamide. After adding 0.2 µg of isotope-labeled [^{15}N]APOA1 (as the internal standard), the serum was incubated at 37°C with 50:1 (w/w, proteins/enzyme) of sequencing grade modified trypsin (Promega, Madison, WI) for 4 h. A second aliquot of trypsin (1:25 final, w/w, enzyme/protein) was added, and the samples were incubated overnight at 37°C. Digestion was halted by acidifying the reaction mixture (pH 2 to 3) with trifluoroacetic acid, and the samples were dried and stored at −80°C until MS analysis.

Mouse plasma digestion. Plasma digestion was performed as follows: 3 µL of plasma was diluted 20x in 100 mM NH_4HCO_3, 10 µL of diluted plasma was diluted to 50 µL with 0.625% sodium deoxycholate (SDC) in 100 mM NH_4HCO_3 and spiked with 0.05 µg of ^{15}N-APOA1, reduced with dithiotreitol (DTT) (30 min at 60°C), and then alkylated with iodoacetamide (IAA) (45 min at room temperature in the dark). Excess IAA was quenched with additional DTT and the sample was digested with 3 µg of sequencing grade trypsin (Promega; ~ 1:10 w/w to plasma protein). SDC was precipitated by addition of 5 µL of 20% trifluoroacetic acid and precipitates were spun down. 60 µL was transferred into a PCR plate and frozen at -20°C until analysis.

Quantification of human serum APOC3 by parallel reaction monitoring with ^{15}N-labeled APOA1. To quantitatively measure the relative levels of APOC3 in serum, we used targeted proteomics with parallel reaction monitoring (PRM) that quantifies multiple proteins as accurately as selected reaction monitoring (SRM) and biochemical approaches (58). A nanoACQUITY UPLC (Waters, Milford, MA) was used for the separation, with a linear gradient of 0.1% formic acid in water (solvent A) and 0.1% formic acid in acetonitrile (solvent B). After the dried peptide digests were reconstituted in 0.1% formic acid, serum peptide digests (equivalent to 0.2 µg of protein) were desalted on a C18 trap column (0.1 × 40 mm) packed in house with Magic C-18 reverse-phase resin (5 µm; 100 Å; Michrom Bioresources) for 8 min at 2.5 µL/min in 99% solvent A, and then separated using a C-18

analytical column (0.1 × 150 mm) packed in-house with Magic C-18 reverse-phase resin (5 µm; 100 Å; Michrom Bioresources) with an uncoated SilicaTip Emitters (20 µm ID, 10 µm tip ID; New Objective, Woburn, MA). The column was kept at 50°C and the peptides were eluted from the trap column onto the analytical column at a flow rate of 0.6 µL/min and separated using multistep gradient as follows: 1% to 7% solvent B in 1 min; 7% to 25% solvent B in 27 min; and 25% to 35% solvent B in 8 min. The column was subsequently washed for 3 min at 80% solvent B and re-equilibrated at 99% solvent A for 12 min. Peptide digests were analyzed with an ultrahigh-resolution accurate mass Orbitrap Fusion Lumos Tribrid Mass Spectrometer (Thermo Fisher Scientific, San Jose, CA). The mass spectrometer was operated in data-independent acquisition PRM mode. A survey full scan MS (from m/z 350-1800) was acquired in the Orbitrap at a resolution of 120,000 at 400 m/z. A targeted list of precursor ions with charge state 2 or 3 were isolated and fragmented using higher energy collisional dissociation fragmentation with 30% collision energy with a stepped collision energy of 5% and detected at a mass resolution of 15,000 at 400 m/z with a maximum injection time of 20 ms and automated gain control target of 10,000.

Targeted proteomics data analysis of human serum. Two peptides of APOC3 were selected for quantitative analysis by PRM (59). The MS data were analyzed with Skyline, an open source program (60), to determine the total peak area of all the transitions detected for each peptide. The relative levels of each peptide were calculated by the ratio of the total peak area of all the transitions for each peptide

to the total peak area of all the transitions for [^{15}N]THLAPYSDELR (the internal standard peptide derived from [^{15}N]APOA1) (59). To calculate the relative levels of the peptide between cohort and CAD groups, we set the average ratio of the peptide in control subjects to an arbitrary unit of one. To obtain the relative levels of APOC3, the relative levels of the two peptides from the protein were averaged.

Mouse plasma targeted proteomics analysis. The abundance of the selected mouse plasma proteins was quantified by mass spectrometry using targeted proteomics. Recombinant mouse APOC3 was used as a standard for mouse APOC3 plasma analysis. Tryptic digests were desalted on a C18 trapping column (Reprosil-Pur 120 C18-AQ, 5 µm, 0.1 x 40 mm, Dr. Maisch HPLC GmbH, Ammerbuch-Entringen, Germany) (trapping flow rate 4 µL/min), and separated on a capillary analytical column (Reprosil-Pur 120 C18-AQ, 5 µm, 250x0.075 mm, Dr. Maisch HPLC GmbH) with a 30 min linear gradient of acetonitrile, 0.1% formic acid (7-35%) in 0.1% formic acid in water at a flow rate of 0.4 µL/min using a nanoAquity UPLC (Waters, MA). The mass spectrometric analysis was done on either a Thermo TSQ Vantage (Thermo Fisher) triple-quadrupole mass spectrometer in selected reaction monitoring (SRM) mode, or on Thermo Orbitrap Fusion in the parallel reaction monitoring (PRM) mode. For SRM the instrument was operated with 10 ms dwell time and the selected transitions for the peptide of interest were monitored with collision energies optimized to maximize the signal. For the PRM analysis the instrument was operated at targeted mode with 2 Th precursor selection in the quadrupole analyzer and MS/MS mode with higher energy

collisional dissociation activation (30% normalized collision energy), 30,000 resolution, maximum injection time 54 ms, and automated gain control target 5 x 10^4.

Statistical analyses. Statistical analyses of the mouse data were performed using GraphPad Prism 7.0 (La Jolla, CA). We used two-tailed unpaired Student's *t*-tests to compare differences between two groups. To compare three or more groups, we used either one-way ANVOA or two-way ANOVA followed by Tukey's or Bonferroni post hoc tests, respectively, as indicated in each figure legend. D'Agostino-Pearson omnibus normality tests were performed to evaluate if the data were normally distributed. Statistical outliers were identified by the ROUT (Q=1%) method. Statistical outliers were removed in Figure 6D and Figure S6B, as indicated in the figure legends. Data not normally distributed were analyzed by Kruskal-Wallis tests followed by Dunn's multiple comparison tests (multiple groups) or Mann-Whitney tests (two groups). A *p*-value of <0.05 was considered statistically significant.

Study approval. All human subjects provided informed consent, and the study was approved by the Colorado Combined Institutional Review Board, protocol #97-661. The animal experiments were performed in accordance with an approved University of Washington Institutional Animal Care and Use Committee protocol (protocol # 3154-01) or an approved Columbia University Institutional Animal Care and Use Committee protocol (protocol # AAAQ4433).

Funding. This study was supported by NIH grants R01HL126028, DP3DK108209, R01HL127694, and P01HL092969 (KEB). Part of the study was supported by the Diabetes Research Center at the University of Washington, P30DK017047, and the American Diabetes Association grant 1-16-IBS-153 (JEK).

Author Contributions. K.E.B. and J.W.H. designed and directed the study. J.E.K, T.V., B.S., J.W.H., and K.E.B analyzed data and wrote the manuscript. M.J.G., R.M.C., B.S., R.A.H., and T.V. contributed to the study design and manuscript preparation. J.E.K., F.K., S.B., B.S., M.S-A., C.R.M., D.M., K.B., and T.V. performed experiments. J.K.S-B., J.E.H., and G.L.K. collected data in the CACTI study and analyzed the CACTI cohort CAD data. All authors reviewed the manuscript and provided final approval for submission.

Table 1. **Clinical characteristics of subjects in CACTI selected for the present study.** Values are shown as mean (SD) or number of patients (%), as indicated. The total number of subjects included was 181 (11 CAD cases were included in the cohort group consisting of 145 subjects).

Covariate	T1DM cohort	T1DM CAD cases	HR (95% CI)	p-value
Number of subjects	145	47		
Age (years)	37.0 (9.0)	43.6 (7.9)	1.10 (1.06, 1.15)	<0.0001
Sex (female)	79 (54.5%)	21 (44.7%)	0.67 (0.35, 1.29)	0.23
Duration (years)	23.4 (8.2)	30.6 (7.7)	1.13 (1.08, 1.19)	<0.0001
SBP (mmHg)	118.5 (15.6)	126.3 (15.0)	1.03 (1.02, 1.05)	0.0002
DBP (mmHg)	77.7 (9.1)	81.1 (9.4)	1.05 (1.02,1.08)	0.001
BMI (kg/m^2)	26.3 (4.4)	27.3 (5.2)	1.05 (0.98, 1.13)	0.17
Total cholesterol (mg/dL)	170.5 (337)	185.7 (30.7)	1.1 (1.01, 1.02)	0.002
Triglycerides (mg/dL)*	75 (58-103)	99 (72-132)	2.26 (1.40, 3.65)	0.0009
HDL-C (mg/dL)	55.0 (16.0)	57.0 (19.2)	1.01 (0.98, 1.03)	0.53
LDL-C (mg/dL)	96.5 (28.2)	105.7 (29.7)	1.01 (1.00, 1.03)	0.03
HbA1c (%)	7.7 (1.2)	8.4 (1.1)	1.42 (1.15, 1.75)	0.001
Insulin dose per body weight (units/kg/day)	0.65 (0.29)	0.62 (0.30)	0.74 (0.16, 3.40)	0.70
CRP ($\mu g/mL$)*	1.2 (0.9-2.0)	1.4 (0.9-2.6)	1.43 (0.89, 2.28)	0.14
eGFR ($mL/min/1.73m^2$)	104.5 (25.2)	79.6 (34.6)	0.97 (0.96, 0.98)	<0.0001
Current smoker	17 (11.8%)	14 (29.8%)	3.40 (1.54, 7.48)	0.002
Medications				
ACE inhibitor	52 (35.9%)	27 (57.4%)	2.58 (1.34, 4.97)	0.005
Angiotensin II receptor blocker	6 (4.1%)	4 (8.5%)	2.35 (0.62, 8.96)	0.21
Antihypertensive	60 (41.4%)	35 (74.5%)	4.6 (2.3, 9.5)	<0.0001
Statin	24 (16.6%)	24 (51.1%)	5.3 (2.7, 10.5)	<0.0001

* Median and IQR

References

1. Emerging Risk Factors C, Sarwar N, Gao P, Seshasai SR, Gobin R, Kaptoge S, et al. Diabetes mellitus, fasting blood glucose concentration, and risk of vascular disease: a collaborative meta-analysis of 102 prospective studies. *Lancet.* 2010;375(9733):2215-22.

2. Rawshani A, Rawshani A, Franzen S, Eliasson B, Svensson AM, Miftaraj M, et al. Mortality and Cardiovascular Disease in Type 1 and Type 2 Diabetes. *N Engl J Med.* 2017;376(15):1407-18.

3. Laakso M, and Kuusisto J. Insulin resistance and hyperglycaemia in cardiovascular disease development. *Nat Rev Endocrinol.* 2014;10(5):293-302.

4. Lachin JM, Orchard TJ, Nathan DM, and Group DER. Update on cardiovascular outcomes at 30 years of the diabetes control and complications trial/epidemiology of diabetes interventions and complications study. *Diabetes Care.* 2014;37(1):39-43.

5. Nathan DM, McGee P, Steffes MW, Lachin JM, and Group DER. Relationship of glycated albumin to blood glucose and HbA1c values and to retinopathy, nephropathy, and cardiovascular outcomes in the DCCT/EDIC study. *Diabetes.* 2014;63(1):282-90.

6. Writing Group for the DERG, Orchard TJ, Nathan DM, Zinman B, Cleary P, Brillon D, et al. Association between 7 years of intensive treatment of type 1 diabetes and long-term mortality. *JAMA.* 2015;313(1):45-53.

7. Bebu I, Braffett BH, Pop-Busui R, Orchard TJ, Nathan DM, Lachin JM, et al. The relationship of blood glucose with cardiovascular disease is mediated

over time by traditional risk factors in type 1 diabetes: the DCCT/EDIC study. *Diabetologia.* 2017;60(10):2084-91.

8. Cooper ME, El-Osta A, Allen TJ, Watson AMD, Thomas MC, and Jandeleit-Dahm KAM. Metabolic Karma-The Atherogenic Legacy of Diabetes: The 2017 Edwin Bierman Award Lecture. *Diabetes.* 2018;67(5):785-90.

9. Shah MS, and Brownlee M. Molecular and Cellular Mechanisms of Cardiovascular Disorders in Diabetes. *Circ Res.* 2016;118(11):1808-29.

10. Bornfeldt KE. Does Elevated Glucose Promote Atherosclerosis? Pros and Cons. *Circ Res.* 2016;119(2):190-3.

11. Chait A, and Bornfeldt KE. Diabetes and atherosclerosis: is there a role for hyperglycemia? *J Lipid Res.* 2009;50 Suppl:S335-9.

12. Chen M, Breslow JL, Li W, and Leff T. Transcriptional regulation of the apoC-III gene by insulin in diabetic mice: correlation with changes in plasma triglyceride levels. *J Lipid Res.* 1994;35(11):1918-24.

13. Li WW, Dammerman MM, Smith JD, Metzger S, Breslow JL, and Leff T. Common genetic variation in the promoter of the human apo CIII gene abolishes regulation by insulin and may contribute to hypertriglyceridemia. *J Clin Invest.* 1995;96(6):2601-5.

14. Taskinen MR, and Boren J. Why Is Apolipoprotein CIII Emerging as a Novel Therapeutic Target to Reduce the Burden of Cardiovascular Disease? *Curr Atheroscler Rep.* 2016;18(10):59.

15. Pollin TI, Damcott CM, Shen H, Ott SH, Shelton J, Horenstein RB, et al. A null mutation in human APOC3 confers a favorable plasma lipid profile and apparent cardioprotection. *Science.* 2008;322(5908):1702-5.

16. Saleheen D, Natarajan P, Armean IM, Zhao W, Rasheed A, Khetarpal SA, et al. Human knockouts and phenotypic analysis in a cohort with a high rate of consanguinity. *Nature.* 2017;544(7649):235-9.

17. Tg, Hdl Working Group of the Exome Sequencing Project NHL, Blood I, Crosby J, Peloso GM, Auer PL, et al. Loss-of-function mutations in APOC3, triglycerides, and coronary disease. *N Engl J Med.* 2014;371(1):22-31.

18. Jorgensen AB, Frikke-Schmidt R, Nordestgaard BG, and Tybjaerg-Hansen A. Loss-of-function mutations in APOC3 and risk of ischemic vascular disease. *N Engl J Med.* 2014;371(1):32-41.

19. Khetarpal SA, Zeng X, Millar JS, Vitali C, Somasundara AVH, Zanoni P, et al. A human APOC3 missense variant and monoclonal antibody accelerate apoC-III clearance and lower triglyceride-rich lipoprotein levels. *Nat Med.* 2017;23(9):1086-94.

20. Pechlaner R, Tsimikas S, Yin X, Willeit P, Baig F, Santer P, et al. Very-Low-Density Lipoprotein-Associated Apolipoproteins Predict Cardiovascular Events and Are Lowered by Inhibition of APOC-III. *J Am Coll Cardiol.* 2017;69(7):789-800.

21. Larsson M, Allan CM, Jung RS, Heizer PJ, Beigneux AP, Young SG, et al. Apolipoprotein C-III inhibits triglyceride hydrolysis by GPIHBP1-bound LPL. *J Lipid Res.* 2017;58(9):1893-902.

22. Gaudet D, Brisson D, Tremblay K, Alexander VJ, Singleton W, Hughes SG, et al. Targeting APOC3 in the familial chylomicronemia syndrome. *N Engl J Med.* 2014;371(23):2200-6.

23. Gordts PL, Nock R, Son NH, Ramms B, Lew I, Gonzales JC, et al. ApoC-III inhibits clearance of triglyceride-rich lipoproteins through LDL family receptors. *J Clin Invest.* 2016;126(8):2855-66.

24. Reyes-Soffer G SC, Horenstein RB, Holleran S, Matveyenko A, Thomas T, Nandakumar R, Ngai C, Karmally W, Ginsberg HN, Ramakrishnan R, Pollin TI. Effects of APOC3 Heterozygous Deficiency on Plasma Lipid and Lipoprotein Metabolism. *Arterioscler Thromb Vasc Biol.* 2018;E-Pub Ahead of Print.

25. Ramms B, Patel S, Nora C, Pessentheiner AR, Chang MW, Green CR, et al. ApoC-III ASO Promotes Tissue LPL Activity in Absence of ApoE-Mediated TRL Clearance. *J Lipid Res.* 2019.

26. Ginsberg HN. Lipoprotein physiology in nondiabetic and diabetic states. Relationship to atherogenesis. *Diabetes Care.* 1991;14(9):839-55.

27. Renard CB, Kramer F, Johansson F, Lamharzi N, Tannock LR, von Herrath MG, et al. Diabetes and diabetes-associated lipid abnormalities have distinct effects on initiation and progression of atherosclerotic lesions. *J Clin Invest.* 2004;114(5):659-68.

28. Johansson F, Kramer F, Barnhart S, Kanter JE, Vaisar T, Merrill RD, et al. Type 1 diabetes promotes disruption of advanced atherosclerotic lesions in LDL receptor-deficient mice. *Proc Natl Acad Sci U S A.* 2008;105(6):2082-7.

29. Wall VZ, Barnhart S, Kramer F, Kanter JE, Vivekanandan-Giri A, Pennathur S, et al. Inflammatory stimuli induce acyl-CoA thioesterase 7 and remodeling of phospholipids containing unsaturated long (>/=C20)-acyl chains in macrophages. *J Lipid Res.* 2017;58(6):1174-85.

30. Caron S, Verrijken A, Mertens I, Samanez CH, Mautino G, Haas JT, et al. Transcriptional activation of apolipoprotein CIII expression by glucose may contribute to diabetic dyslipidemia. *Arterioscler Thromb Vasc Biol.* 2011;31(3):513-9.

31. Altomonte J, Cong L, Harbaran S, Richter A, Xu J, Meseck M, et al. Foxo1 mediates insulin action on apoC-III and triglyceride metabolism. *J Clin Invest.* 2004;114(10):1493-503.

32. Lee SX, Heine M, Schlein C, Ramakrishnan R, Liu J, Belnavis G, et al. FoxO transcription factors are required for hepatic HDL cholesterol clearance. *J Clin Invest.* 2018;128(4):1615-26.

33. Batista TM, Garcia-Martin R, Cai W, Konishi M, O'Neill BT, Sakaguchi M, et al. Multi-dimensional Transcriptional Remodeling by Physiological Insulin In Vivo. *Cell Rep.* 2019;26(12):3429-43 e3.

34. Huff MW, Fidge NH, Nestel PJ, Billington T, and Watson B. Metabolism of C-apolipoproteins: kinetics of C-II, C-III1 and C-III2, and VLDL-apolipoprotein B in normal and hyperlipoproteinemic subjects. *J Lipid Res.* 1981;22(8):1235-46.

35. Graham MJ, Lee RG, Bell TA, 3rd, Fu W, Mullick AE, Alexander VJ, et al. Antisense oligonucleotide inhibition of apolipoprotein C-III reduces plasma

triglycerides in rodents, nonhuman primates, and humans. *Circ Res.* 2013;112(11):1479-90.

36. Sacks FM. The crucial roles of apolipoproteins E and C-III in apoB lipoprotein metabolism in normolipidemia and hypertriglyceridemia. *Curr Opin Lipidol.* 2015;26(1):56-63.

37. Bell TA, 3rd, Graham, MJ, Baker, BF, Crooke, RM. Therapeutic inhibition of apoC-III for the treatment of hypertriglyceridemia. *Clin Lipidol.* 2015;10(2):191-203.

38. Digenio A, Dunbar RL, Alexander VJ, Hompesch M, Morrow L, Lee RG, et al. Antisense-Mediated Lowering of Plasma Apolipoprotein C-III by Volanesorsen Improves Dyslipidemia and Insulin Sensitivity in Type 2 Diabetes. *Diabetes Care.* 2016;39(8):1408-15.

39. Gaudet D, Alexander VJ, Baker BF, Brisson D, Tremblay K, Singleton W, et al. Antisense Inhibition of Apolipoprotein C-III in Patients with Hypertriglyceridemia. *N Engl J Med.* 2015;373(5):438-47.

40. Kanter JE, Kramer F, Barnhart S, Averill MM, Vivekanandan-Giri A, Vickery T, et al. Diabetes promotes an inflammatory macrophage phenotype and atherosclerosis through acyl-CoA synthetase 1. *Proc Natl Acad Sci U S A.* 2012;109(12):E715-24.

41. MacDougall ED, Kramer F, Polinsky P, Barnhart S, Askari B, Johansson F, et al. Aggressive very low-density lipoprotein (VLDL) and LDL lowering by gene transfer of the VLDL receptor combined with a low-fat diet regimen induces

regression and reduces macrophage content in advanced atherosclerotic lesions in LDL receptor-deficient mice. *Am J Pathol.* 2006;168(6):2064-73.

42. Nagareddy PR, Murphy AJ, Stirzaker RA, Hu Y, Yu S, Miller RG, et al. Hyperglycemia promotes myelopoiesis and impairs the resolution of atherosclerosis. *Cell Metab.* 2013;17(5):695-708.

43. Soehnlein O, and Swirski FK. Hypercholesterolemia links hematopoiesis with atherosclerosis. *Trends Endocrinol Metab.* 2013;24(3):129-36.

44. Tall AR, Yvan-Charvet L, Westerterp M, and Murphy AJ. Cholesterol efflux: a novel regulator of myelopoiesis and atherogenesis. *Arterioscler Thromb Vasc Biol.* 2012;32(11):2547-52.

45. Kraakman MJ, Lee MK, Al-Sharea A, Dragoljevic D, Barrett TJ, Montenont E, et al. Neutrophil-derived S100 calcium-binding proteins A8/A9 promote reticulated thrombocytosis and atherogenesis in diabetes. *J Clin Invest.* 2017;127(6):2133-47.

46. Le PT, Muller MT, and Mortensen RF. Acute phase reactants of mice. I. Isolation of serum amyloid P-component (SAP) and its induction by a monokine. *J Immunol.* 1982;129(2):665-72.

47. Williams KJ, and Tabas I. The response-to-retention hypothesis of early atherogenesis. *Arterioscler Thromb Vasc Biol.* 1995;15(5):551-61.

48. Li H, Han Y, Qi R, Wang Y, Zhang X, Yu M, et al. Aggravated restenosis and atherogenesis in ApoCIII transgenic mice but lack of protection in ApoCIII knockouts: the effect of authentic triglyceride-rich lipoproteins with and without ApoCIII. *Cardiovasc Res.* 2015;107(4):579-89.

49. Bomsztyk K, Mar D, Wang Y, Denisenko O, Ware C, Frazar CD, et al. PIXUL-ChIP: integrated high-throughput sample preparation and analytical platform for epigenetic studies. *Nucleic Acids Res.* 2019.

50. Laatsch A, Merkel M, Talmud PJ, Grewal T, Beisiegel U, and Heeren J. Insulin stimulates hepatic low density lipoprotein receptor-related protein 1 (LRP1) to increase postprandial lipoprotein clearance. *Atherosclerosis.* 2009;204(1):105-11.

51. Windler E, and Havel RJ. Inhibitory effects of C apolipoproteins from rats and humans on the uptake of triglyceride-rich lipoproteins and their remnants by the perfused rat liver. *J Lipid Res.* 1985;26(5):556-65.

52. Aalto-Setala K, Fisher EA, Chen X, Chajek-Shaul T, Hayek T, Zechner R, et al. Mechanism of hypertriglyceridemia in human apolipoprotein (apo) CIII transgenic mice. Diminished very low density lipoprotein fractional catabolic rate associated with increased apo CIII and reduced apo E on the particles. *J Clin Invest.* 1992;90(5):1889-900.

53. Kowal RC, Herz J, Weisgraber KH, Mahley RW, Brown MS, and Goldstein JL. Opposing effects of apolipoproteins E and C on lipoprotein binding to low density lipoprotein receptor-related protein. *J Biol Chem.* 1990;265(18):10771-9.

54. Olin-Lewis K, Krauss RM, La Belle M, Blanche PJ, Barrett PH, Wight TN, et al. ApoC-III content of apoB-containing lipoproteins is associated with binding to the vascular proteoglycan biglycan. *J Lipid Res.* 2002;43(11):1969-77.

55. Hiukka A, Stahlman M, Pettersson C, Levin M, Adiels M, Teneberg S, et al. ApoCIII-enriched LDL in type 2 diabetes displays altered lipid composition,

increased susceptibility for sphingomyelinase, and increased binding to biglycan. *Diabetes.* 2009;58(9):2018-26.

56. Dabelea D, Kinney G, Snell-Bergeon JK, Hokanson JE, Eckel RH, Ehrlich J, et al. Effect of type 1 diabetes on the gender difference in coronary artery calcification: a role for insulin resistance? The Coronary Artery Calcification in Type 1 Diabetes (CACTI) Study. *Diabetes.* 2003;52(11):2833-9.

57. Daugherty A, Tall AR, Daemen M, Falk E, Fisher EA, Garcia-Cardena G, et al. Recommendation on Design, Execution, and Reporting of Animal Atherosclerosis Studies: A Scientific Statement From the American Heart Association. *Arterioscler Thromb Vasc Biol.* 2017;37(9):e131-e57.

58. Ronsein GE, Pamir N, von Haller PD, Kim DS, Oda MN, Jarvik GP, et al. Parallel reaction monitoring (PRM) and selected reaction monitoring (SRM) exhibit comparable linearity, dynamic range and precision for targeted quantitative HDL proteomics. *J Proteomics.* 2015;113:388-99.

59. Shao B, de Boer I, Tang C, Mayer PS, Zelnick L, Afkarian M, et al. A Cluster of Proteins Implicated in Kidney Disease Is Increased in High-Density Lipoprotein Isolated from Hemodialysis Subjects. *J Proteome Res.* 2015;14(7):2792-806.

60. MacLean B, Tomazela DM, Shulman N, Chambers M, Finney GL, Frewen B, et al. Skyline: an open source document editor for creating and analyzing targeted proteomics experiments. *Bioinformatics.* 2010;26(7):966-8.

Figure Legends

Figure 1. **Plasma APOC3 is a strong predictor of coronary artery disease events in subjects with type 1 diabetes, and is independent of traditional CAD risk factors.** Hazard ratio (HR) for CAD events per 1 standard deviation increase in log fasting plasma triglycerides (TG) or log serum APOC3, as calculated by Cox proportional-hazards models (47 subjects with events; 181 total subjects). Also shown are 95% confidence intervals (CI) and p-values. A total of 47 participants had a primary end-point coronary artery disease event, defined as a first nonfatal myocardial infarction, coronary revascularization or death from coronary artery disease causes. Model 1 is a model adjusted for age, sex and diabetes duration. Model 2 is model 1 further adjusted for non-lipid risk factors: HbA1c, systolic and diastolic blood pressure and current smoking status. Model 3 is model 1 further adjusted for lipid risk factors: LDL-C and HDL-C. Model 4 is model 1 further adjusted for log fasting TG.

Figure 2. **Diabetes increases APOC3 levels relative to plasma TG levels through a lack of sufficient insulin**. **A**. Female *Ldlr*$^{-/-}$*;Gp*^{Tg} mice were rendered diabetic using lymphocytic choriomeningitis virus (LCMV). Saline was used as control in non-diabetic littermates. At the onset of diabetes, the mice were switched to a low-fat, semi-purified diet and maintained for 4 weeks. Plasma triglycerides (TG) were compared to plasma APOC3 levels measured by ELISA, using data from three separate cohorts of mice (n=42-43). Ranges and averages of TG levels

and blood glucose (mg/dl) in diabetic and non-diabetic mice are listed below the graph. **B**. Diabetes was induced in male *Ldlr*$^{-/-}$;*Gp*^{Tg} mice by streptozotocin. Following induction of diabetes half of the diabetic cohort received the SGLT2 inhibitor dapagliflozin in their drinking water for 4 weeks. **B**. Blood glucose at the end of the study. **C**. Plasma cholesterol. **D**. Plasma TGs. **E.** Plasma APOC3. (B-E; n=6-8). Diabetes was induced using LCMV in *Ldlr*$^{-/-}$;*Gp*^{Tg} mice. Following development of diabetes, half of the diabetic cohort was subjected to intense insulin therapy with the goal of normalizing blood glucose whereas the other half was maintained on traditional insulin therapy. **F**. Blood glucose at the end of the study. **G**. Plasma cholesterol. **H**. Plasma TGs. **I**. Plasma APOC3 (F-I; n=5-6), ND, non-diabetic mice; D, diabetic mice. D+int. ins, intense insulin therapy. *p<0.05, **p<0.01, ***p<0.001, two-tailed unpaired Student's t-test (A) or one-way ANOVA followed by Tukey's multiple comparisons tests (B-I).

Figure 3. **Reducing APOC3 expression by an antisense oligonucleotide normalizes TRL levels in diabetic mice**. Female *Ldlr*$^{-/-}$;*Gp*^{Tg} mice were rendered diabetic (D) using LCMV. Saline was used as control in non-diabetic (ND) mice. The mice were maintained for 12 weeks. At the onset of diabetes animals were switched to a low-fat, semi-purified diet. The mice were treated twice/week with 25 mg/kg (intraperitoneal injections) of antisense to Apoc3 (Apoc3 ASO) or a control antisense (cASO) starting 2 days after the onset of diabetes. Doses were adjusted every 2 weeks based on body weight. Animals were bled every 4 weeks for glucose and lipid measurements. **A**. Blood glucose. **B**. Plasma cholesterol. Note that time

point 0 is before animals were initiated on the low-fat semi-purified diet but after they had developed diabetes. **C**. Plasma triglycerides (A-C; n=16-20). **D**. Liver mRNA was isolated and *Apoc3* mRNA was measured by real-time PCR (n=6-18). **E-F.** At the end of the study cholesterol and triglyceride lipoprotein profiles were analyzed in a subset (n=4) of mice. **G**. Plasma levels of APOC3, measured by ELISA (n=12-16) at the end of the study. **H**. The APOC3 ELISA was validated by targeted mass spectrometry (MS) (n=5-6). *p<0.05, **p<0.01, ***p<0.001, unless otherwise indicated, one-way ANOVA followed by Tukey's multiple comparison tests (D,G-H) or two-way ANOVA followed by Bonferroni's multiple comparison tests (A-C, E-F).

Figure 4. **Diabetes results in increased plasma levels of APOE, which are normalized by Apoc3 ASO treatment.** Diabetes (D) was induced in female *Ldlr*$^{-/-}$*;Gp*^{Tg} mice using LCMV. Saline was used as control in non-diabetic (ND) mice. The mice were maintained for 12 weeks and treated with control antisense (cASO) or antisense to Apoc3 (Apoc3 ASO). At the end of the study plasma levels of APOE (**A**), APOB100 (**B**), APOB100+APOB48 (**C**), APOA1 (**D**), APOA4 (**E**) and APOC2 (**F**) were measured by targeted mass spectrometry. The results are expressed as arbitrary units (AU). N=4-5, *p<0.05, **p<0.01, ***p<0.001, one-way ANOVA followed by Tukey's multiple comparison tests.

Figure 5. **Diabetes-accelerated atherosclerosis is prevented by Apoc3 ASO treatment.** Female *Ldlr*$^{-/-}$*;Gp*^{Tg} mice were rendered diabetic (D) using LCMV.

Saline was used as control in non-diabetic (ND) mice. The mice were maintained for 12 weeks. At the onset of diabetes the mice were switched to a low-fat, semi-purified diet. Animals were treated twice/week with 25 mg/kg (intraperitoneal injections) of antisense to Apoc3 (Apoc3 ASO) or a control antisense (cASO) starting 2 days after the onset of diabetes. **A, D**. *En face* aortic atherosclerosis (n=15-19). **B-C**. Examples of early lesions in the brachiocephalic artery (BCA). Insert is showing Mac-2 staining. The internal elastic lamina is indicated by arrows. **E**. Quantification of the maximal lesion area in BCA (n=9-11). **F**. Mac-2-positive lesion area in BCA cross-sections (n=7-11). **G**. Quantification of APOC3 immunoreactivity in the BCA (n=3-8). **H**. Quantification of APOE immunoreactivity in the BCA (n=6-11). **I**. Quantification of APOB immunoreactivity in the BCA (n=7-11) *p<0.05, **p<0.01, ***p<0.001, one-way ANOVA followed by Tukey's multiple comparison tests. Scale bar is 0.5 cm in A and 100 μm in B and C.

Figure 6. **Diabetes increases APOC3 levels in interstitial fluid concomitant with macrophage cholesteryl ester accumulation, and this is prevented by the Apoc3 ASO.** Female *Ldlr*$^{-/-}$*;Gp*^{Tg} mice were rendered diabetic (D) using LCMV. Saline was used as control in non-diabetic (ND) mice. The mice were maintained for 4 weeks. At the onset of diabetes, animals were switched to a low-fat, semi-purified diet. The mice were treated twice/week with 25 mg/kg (intraperitoneal injections) of antisense to Apoc3 (Apoc3 ASO) or a control antisense (cASO) starting 2 days after the onset of diabetes. At the end of the study resident macrophages were isolated by peritoneal lavage and the interstitial peritoneal fluid

was collected. **A**. Total macrophage cholesterol. **B**. Macrophage cholesteryl ester (CE). **C**. Cholesterol levels in peritoneal fluid. **D**. APOC3 levels in peritoneal fluid. A-D; N=10-14 (2 statistical outliers were removed from B; 1 in the ND Apoc3 ASO group and 1 in the D cASO group), *p<0.05, **p<0.01, ***p<0.001, one-way ANOVA followed by Tukey's multiple comparison tests.

Figure 7. **Apoc3 ASO treatment reduces necrotic cores in pre-existing lesions in diabetic mice.** Female *Ldlr*$^{-/-}$*;Gp*^{Tg} mice were fed a high-fat diet containing 1.25% cholesterol for 12 weeks, switched to chow for 2 weeks, then injected with LCMV to induce diabetes (D) or saline (non-diabetic; ND). Once diabetic, the mice were maintained for 4 weeks on a low-fat semi-purified diet. The mice were treated twice/week with 25 mg/kg (intraperitoneal injections) of antisense to Apoc3 (Apoc3 ASO) or a control antisense (cASO) starting 2 days after the onset of diabetes. **A**. Blood glucose. **B**. Plasma cholesterol. **C**. Plasma triglycerides (TG). **D**. Plasma APOC3. **E**. Example of aortic sinus lesions stained with Movat's pentachrome stain (top), Mac-2 (middle) and APOC3 immunohistochemistry (bottom). **F**. Quantification of aortic sinus lesion size at +180 μm (largest lesion) after the appearance of all three aortic valve leaflets. No differences in lesion size at 0 or +90 μm. **G**. Quantification of aortic lesion Mac-2 at +180 μm. **H-I**. Quantification of APOC3 immuno-histochemistry at +180 μm. **J-K.** Quantification of aortic lesion necrotic cores at +180 μm. Similar results observed at +90 μm. N=9-10, *p<0.05, **p<0.01, ***p<0.001, t-test. Arrow indicates necrotic core. Scale bar is 100 μm.

Figure 8. **Schematic model**. Suboptimally controlled diabetes associated with relative insulin deficiency increases hepatic APOC3 production and to a larger extent plasma APOC3 levels. The increased levels of APOC3 prevent clearance of plasma TLRs (triglyceride-rich lipoproteins) and their remnant lipoproteins (RLPs). As a result, lipoproteins containing APOC3, APOE and APOB accumulate in the artery wall and accelerate macrophage accumulation, foam cell formation, atherogenesis, and coronary artery disease (CAD) risk.

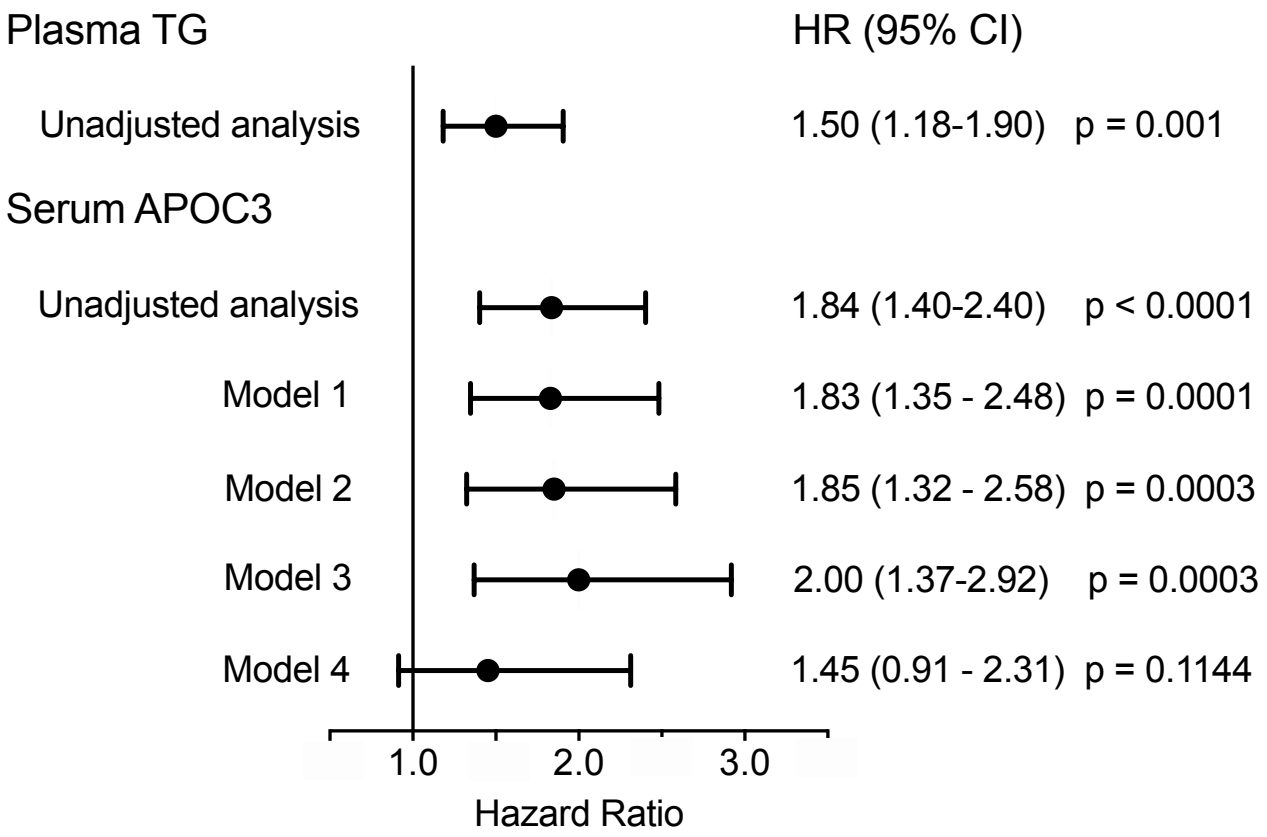

Figure 1. **Plasma APOC3 is a strong predictor of coronary artery disease events in subjects with type 1 diabetes, and is independent of traditional CAD risk factors.** Hazard ratio (HR) for CAD events per 1 standard deviation increase in log fasting plasma triglycerides (TG) or log serum APOC3, as calculated by Cox proportional-hazards models (47 subjects with events; 181 total subjects). Also shown are 95% confidence intervals (CI) and p-values. A total of 47 participants had a primary end-point coronary artery disease event, defined as a first nonfatal myocardial infarction, coronary revascularization or death from coronary artery disease causes. Model 1 is a model adjusted for age, sex and diabetes duration. Model 2 is model 1 further adjusted for non-lipid risk factors: HbA1c, systolic and diastolic blood pressure and current smoking status. Model 3 is model 1 further adjusted for lipid risk factors: LDL-C and HDL-C. Model 4 is model 1 further adjusted for log fasting TG.

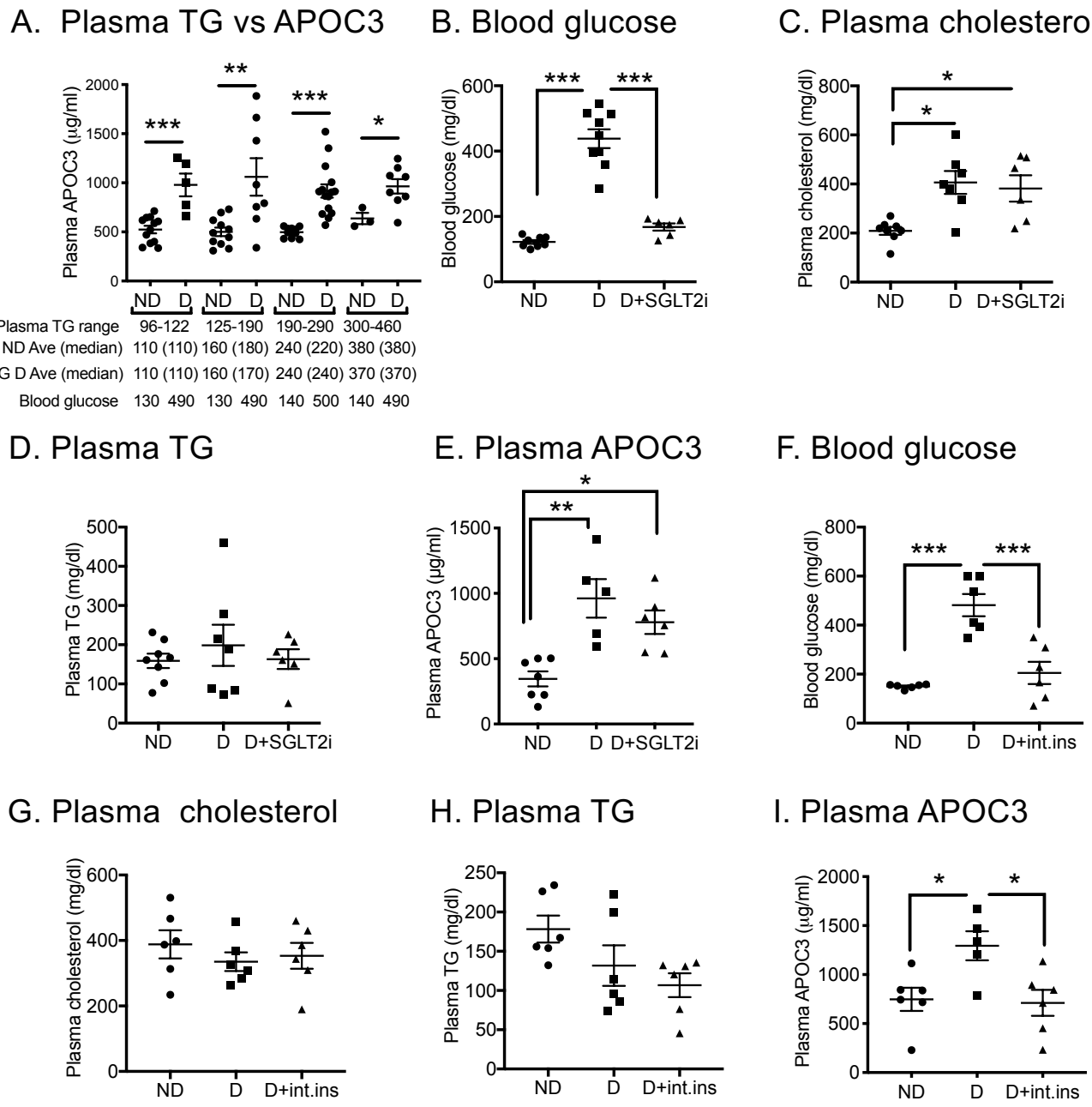

Figure 2. **Diabetes increases APOC3 levels relative to plasma TG levels through a lack of sufficient insulin**. **A**. Female *Ldlr$^{-/-}$;Gp^{Tg}* mice were rendered diabetic using lymphocytic choriomeningitis virus (LCMV). Saline was used as control in non-diabetic littermates. At the onset of diabetes, the mice were switched to a low-fat, semi-purified diet and maintained for 4 weeks. Plasma triglycerides (TG) were compared to plasma APOC3 levels measured by ELISA, using data from three separate cohorts of mice (n=42-43). Ranges and averages of TG levels and blood glucose (mg/dl) in diabetic and non-diabetic mice are listed below the graph. **B**. Diabetes was induced in male *Ldlr$^{-/-}$;Gp^{Tg}* mice by streptozotocin. Following induction of diabetes half of the diabetic cohort received the SGLT2 inhibitor dapagliflozin in their drinking water for 4 weeks. **B**. Blood glucose at the end of the study. **C**. Plasma cholesterol. **D**. Plasma TGs. **E.** Plasma APOC3. (B-E; n=6-8). Diabetes was induced using LCMV in *Ldlr$^{-/-}$;Gp^{Tg}* mice. Following development of diabetes, half of the diabetic cohort was subjected to intense insulin therapy with the goal of normalizing blood glucose whereas the other half was maintained on traditional insulin therapy. **F**. Blood glucose at the end of the study. **G**. Plasma cholesterol. **H**. Plasma TGs. **I**. Plasma APOC3 (F-I; n=5-6), ND, non-diabetic mice; D, diabetic mice. D+int. ins, intense insulin therapy. *p<0.05, **p<0.01, ***p<0.001, two-tailed unpaired Student's t-test (A) or one-way ANOVA followed by Tukey's multiple comparisons tests (B-I).

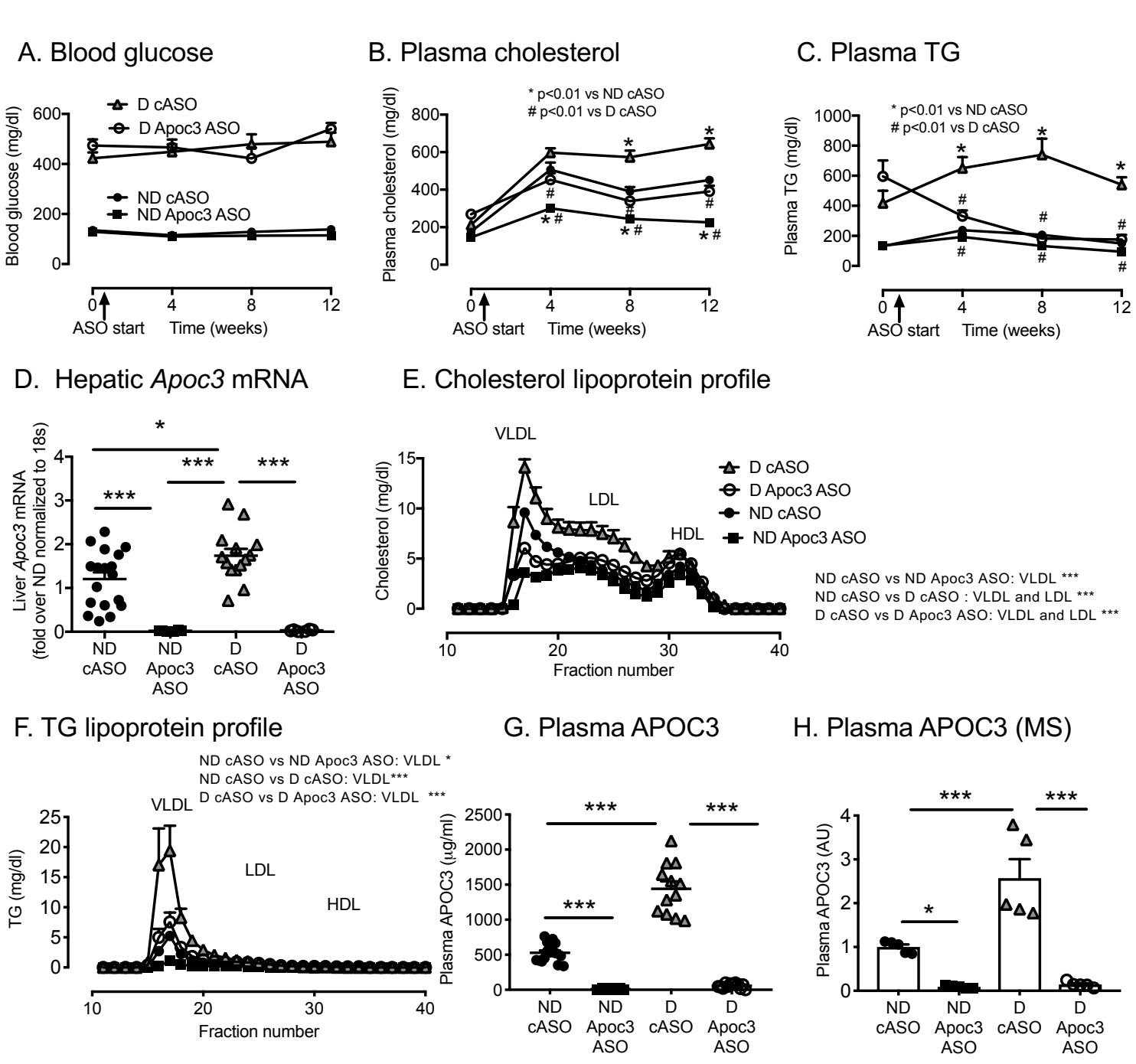

Figure 3. **Reducing APOC3 expression by an antisense oligonucleotide normalizes TRL levels in diabetic mice**. Female *Ldlr*$^{-/-}$*;Gp*^{Tg} mice were rendered diabetic (D) using LCMV. Saline was used as control in non-diabetic (ND) mice. The mice were maintained for 12 weeks. At the onset of diabetes animals were switched to a low-fat, semi-purified diet. The mice were treated twice/week with 25 mg/kg (intraperitoneal injections) of antisense to Apoc3 (Apoc3 ASO) or a control antisense (cASO) starting 2 days after the onset of diabetes. Doses were adjusted every 2 weeks based on body weight. Animals were bled every 4 weeks for glucose and lipid measurements. **A**. Blood glucose. **B**. Plasma cholesterol. Note that time point 0 is before animals were initiated on the low-fat semi-purified diet but after they had developed diabetes. **C**. Plasma triglycerides (A-C; n=16-20). **D**. Liver mRNA was isolated and *Apoc3* mRNA was measured by real-time PCR (n=6-18). **E-F.** At the end of the study cholesterol and triglyceride lipoprotein profiles were analyzed in a subset (n=4) of mice. **G**. Plasma levels of APOC3, measured by ELISA (n=12-16) at the end of the study. **H**. The APOC3 ELISA was validated by targeted mass spectrometry (MS) (n=5-6). *p<0.05, **p<0.01, ***p<0.001, unless otherwise indicated, one-way ANOVA followed by Tukey's multiple comparison tests (D,G-H) or two-way ANOVA followed by Bonferroni's multiple comparison tests (A-C, E-F).

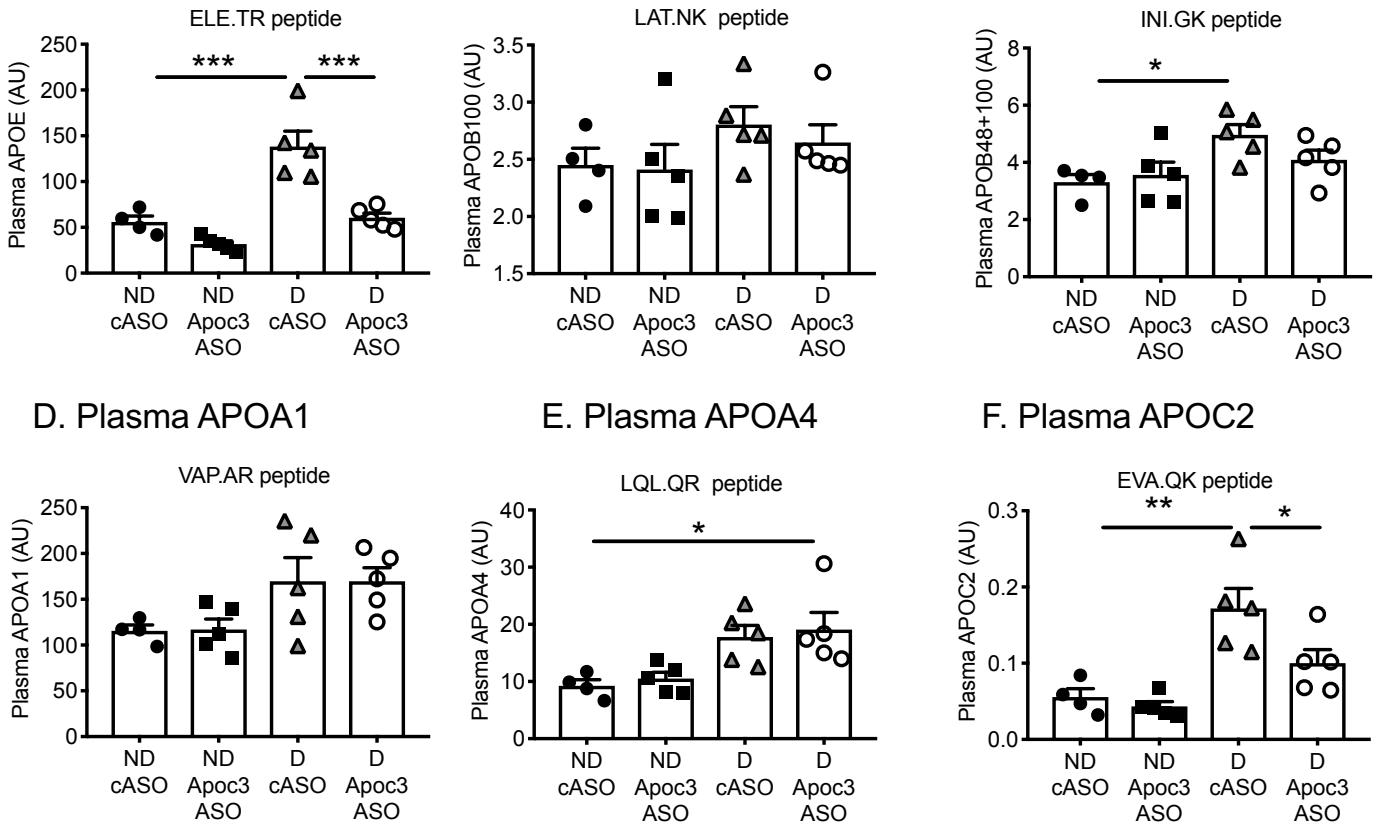

Figure 4. **Diabetes results in increased plasma levels of APOE, which are normalized by Apoc3 ASO treatment.** Diabetes (D) was induced in female *Ldlr*$^{-/-}$*;Gp*^{Tg} mice using LCMV. Saline was used as control in non-diabetic (ND) mice. The mice were maintained for 12 weeks and treated with control antisense (cASO) or antisense to Apoc3 (Apoc3 ASO). At the end of the study plasma levels of APOE (**A**), APOB100 (**B**), APOB100+APOB48 (**C**), APOA1 (**D**), APOA4 (**E**) and APOC2 (**F**) were measured by targeted mass spectrometry. The results are expressed as arbitrary units (AU). N=4-5, *p<0.05, **p<0.01, ***p<0.001, one-way ANOVA followed by Tukey's multiple comparison tests.

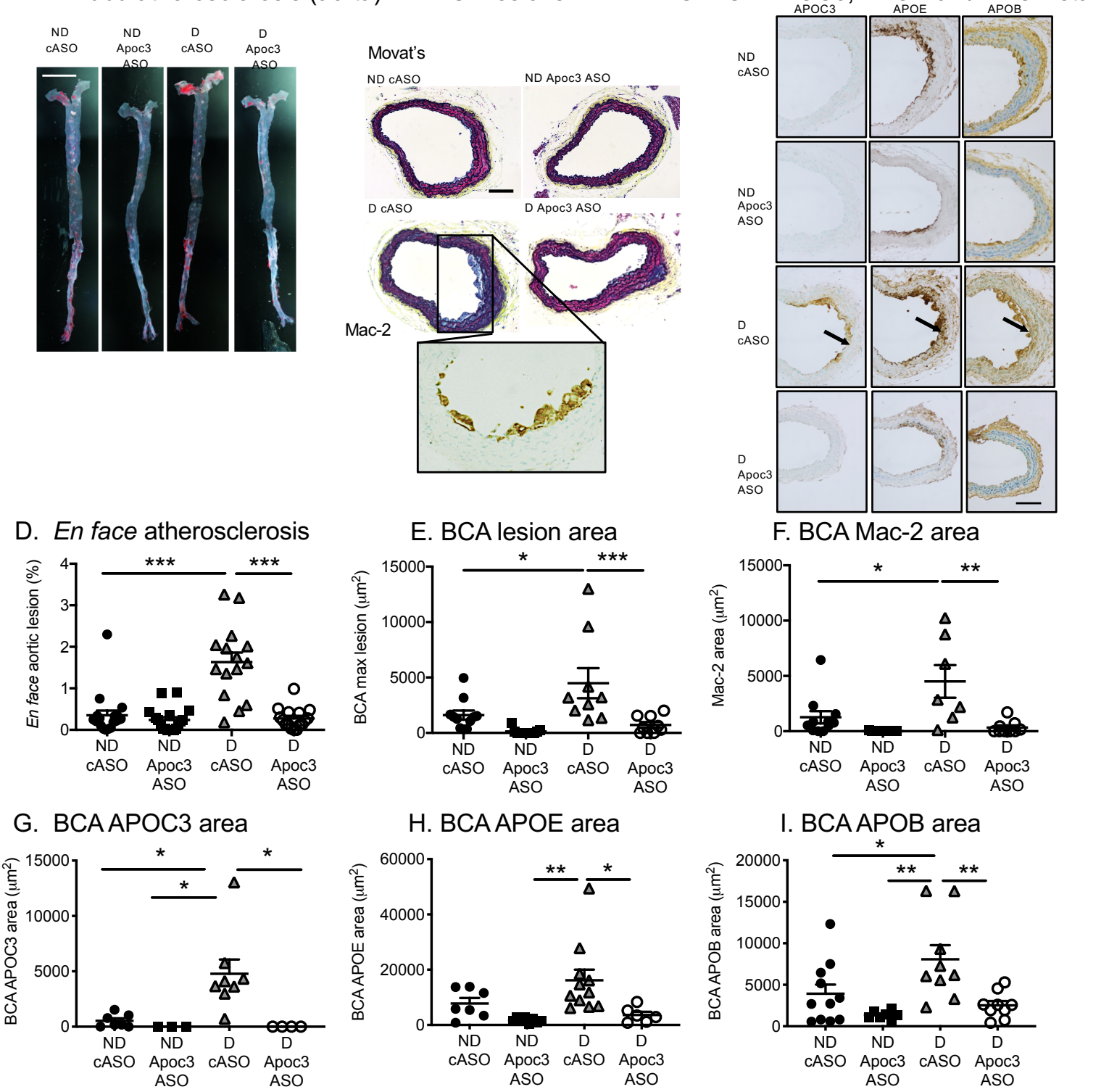

Figure 5. **Diabetes-accelerated atherosclerosis is prevented by Apoc3 ASO treatment.** Female *Ldlr*$^{-/-}$*;Gp*^{Tg} mice were rendered diabetic (D) using LCMV. Saline was used as control in non-diabetic (ND) mice. The mice were maintained for 12 weeks. At the onset of diabetes the mice were switched to a low-fat, semi-purified diet. Animals were treated twice/week with 25 mg/kg (intraperitoneal injections) of antisense to Apoc3 (Apoc3 ASO) or a control antisense (cASO) starting 2 days after the onset of diabetes. **A, D**. *En face* aortic atherosclerosis (n=15-19). **B-C**. Examples of early lesions in the brachiocephalic artery (BCA). Insert is showing Mac-2 staining. The internal elastic lamina is indicated by arrows. **E**. Quantification of the maximal lesion area in BCA (n=9-11). **F**. Mac-2-positive lesion area in BCA cross-sections (n=7-11). **G**. Quantification of APOC3 immunoreactivity in the BCA (n=3-8). **H**. Quantification of APOE immunoreactivity in the BCA (n=6-11). **I**. Quantification of APOB immunoreactivity in the BCA (n=7-11) *p<0.05, **p<0.01, ***p<0.001, one-way ANOVA followed by Tukey's multiple comparison tests. Scale bar is 0.5 cm in A and 100 mm in B and C.

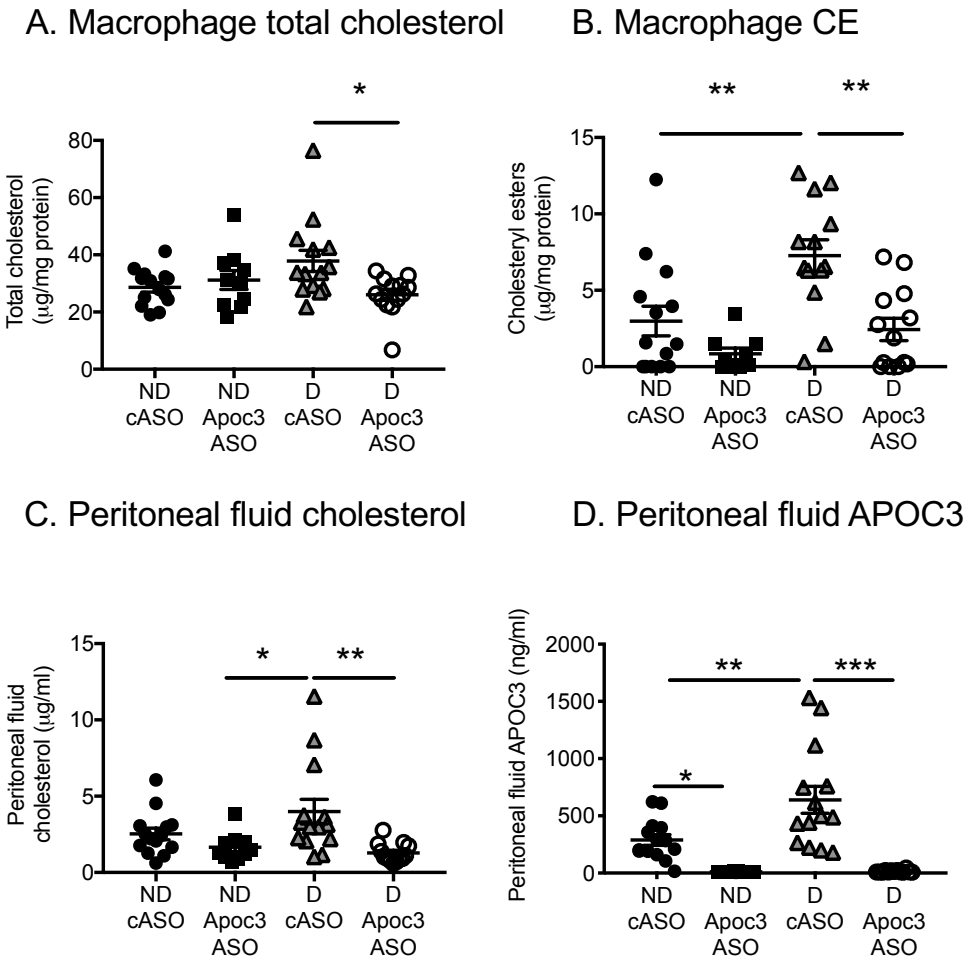

Figure 6. **Diabetes increases APOC3 levels in interstitial fluid concomitant with macrophage cholesteryl ester accumulation, and this is prevented by the Apoc3 ASO.** Female *Ldlr*$^{-/-}$*;Gp*^{Tg} mice were rendered diabetic (D) using LCMV. Saline was used as control in non-diabetic (ND) mice. The mice were maintained for 4 weeks. At the onset of diabetes, animals were switched to a low-fat, semi-purified diet. The mice were treated twice/week with 25 mg/kg (intraperitoneal injections) of antisense to Apoc3 (Apoc3 ASO) or a control antisense (cASO) starting 2 days after the onset of diabetes. At the end of the study resident macrophages were isolated by peritoneal lavage and the interstitial peritoneal fluid was collected. **A**. Total macrophage cholesterol. **B**. Macrophage cholesteryl ester (CE). **C**. Cholesterol levels in peritoneal fluid. **D**. APOC3 levels in peritoneal fluid. A-D; N=10-14 (2 statistical outliers were removed from B; 1 in the ND Apoc3 ASO group and 1 in the D cASO group), *p<0.05, **p<0.01, ***p<0.001, one-way ANOVA followed by Tukey's multiple comparison tests.

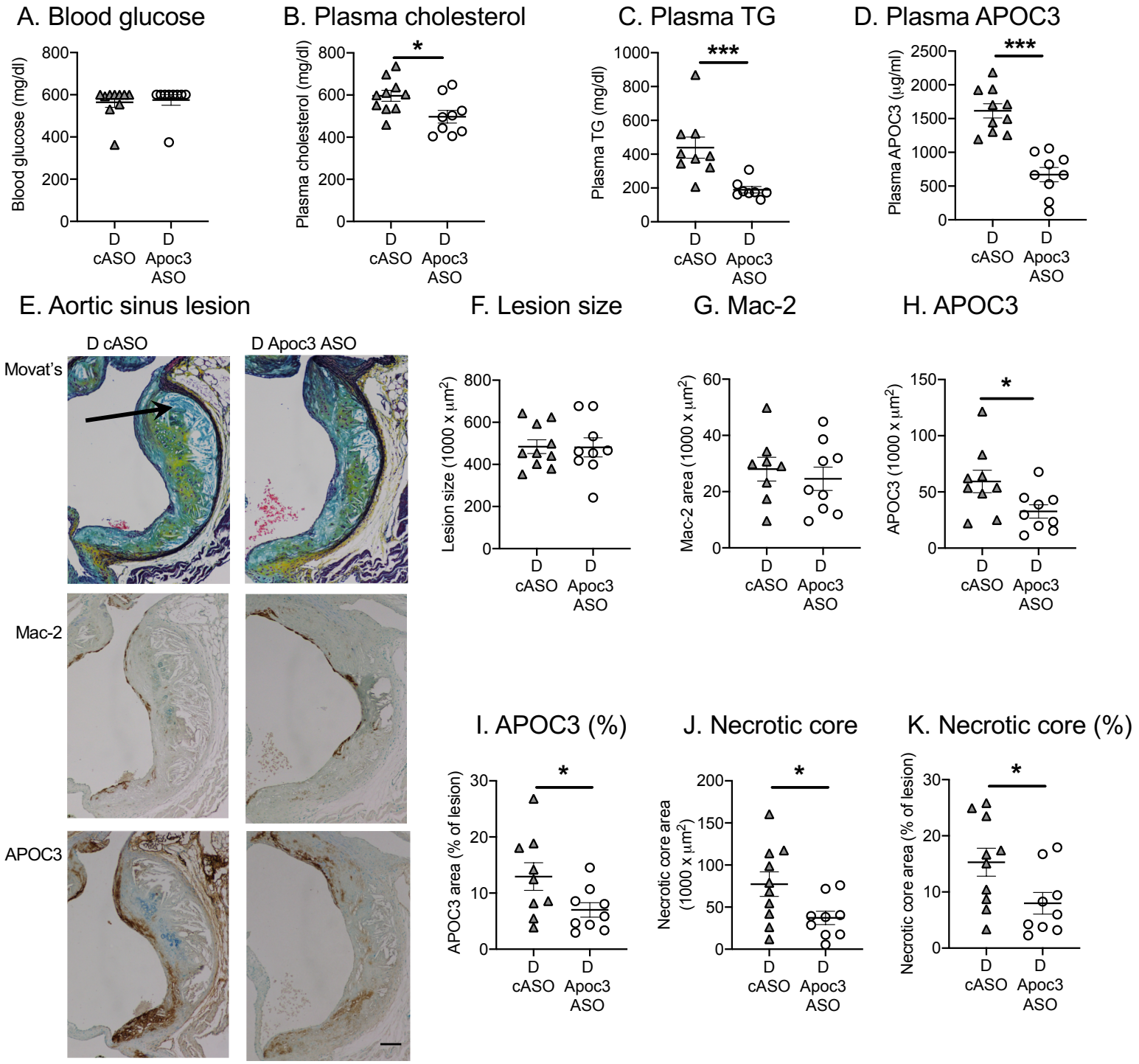

Figure 7. **Apoc3 ASO treatment reduces necrotic cores in pre-existing lesions in diabetic mice.** Female *Ldlr*$^{-/-}$*;Gp*^{Tg} mice were fed a high-fat diet containing 1.25% cholesterol for 12 weeks, switched to chow for 2 weeks, then injected with LCMV to induce diabetes (D) or saline (non-diabetic; ND). Once diabetic, the mice were maintained for 4 weeks on a low-fat semi-purified diet. The mice were treated twice/week with 25 mg/kg (intraperitoneal injections) of antisense to Apoc3 (Apoc3 ASO) or a control antisense (cASO) starting 2 days after the onset of diabetes. **A**. Blood glucose. **B**. Plasma cholesterol. **C**. Plasma triglycerides (TG). **D**. Plasma APOC3. **E**. Example of aortic sinus lesions stained with Movat's pentachrome stain (top), Mac-2 (middle) and APOC3 immunohistochemistry (bottom). **F**. Quantification of aortic sinus lesion size at +180 µm (largest lesion) after the appearance of all three aortic valve leaflets. No differences in lesion size at 0 or +90 µm. **G**. Quantification of aortic lesion Mac-2 at +180 µm. **H-I**. Quantification of APOC3 immuno-histochemistry at +180 µm. **J-K.** Quantification of aortic lesion necrotic cores at +180 µm. Similar results observed at +90 µm. N=9-10, *p<0.05, **p<0.01, ***p<0.001, t-test. Arrow indicates necrotic core. Scale bar is 100 µm.

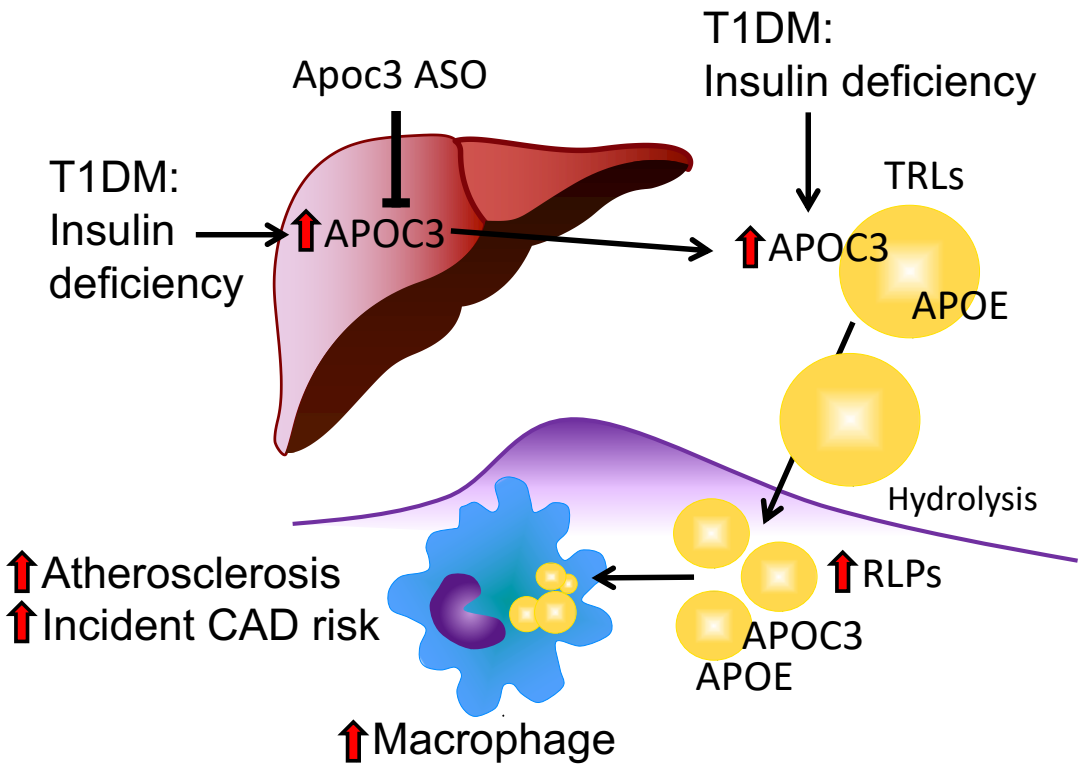

Figure 8. **Schematic model**. Suboptimally controlled diabetes associated with relative insulin deficiency increases hepatic APOC3 production and to a larger extent plasma APOC3 levels. The increased levels of APOC3 prevent clearance of plasma TLRs (triglyceride-rich lipoproteins) and their remnant lipoproteins (RLPs). As a result, lipoproteins containing APOC3, APOE and APOB accumulate in the artery wall and accelerate macrophage accumulation, foam cell formation, atherogenesis, and coronary artery disease (CAD) risk.